

Design, Synthesis, and Kinetic Evaluation of High-Affinity FKBP Ligands and the X-ray Crystal Structures of Their Complexes with FKBP12

Dennis A. Holt,^{*,†} Juan I. Luengo,[†] Dennis S. Yamashita,[†] Hye-Ja Oh,[†]
Arda L. Konialian,[†] Hwa-Kwo Yen,[†] Leonard W. Rozamus,[†] Martin Brandt,[†]
Mary J. Bossard,[†] Mark A. Levy,[†] Drake S. Eggleston,[§] Jun Liang,[§] L. Wayne Schultz,[‡]
Thomas J. Stout,[‡] and Jon Clardy[‡]

Contribution from the Departments of Medicinal Chemistry and Physical & Structural Chemistry, SmithKline Beecham Pharmaceuticals, King of Prussia, Pennsylvania 19406, and Department of Chemistry, Cornell University, Ithaca, New York 14853-1301

Received May 24, 1993*

Abstract: The design and synthesis of high-affinity FKBP12 ligands is described. These compounds potently inhibit the *cis-trans*-peptidylprolyl isomerase (rotamase) activity catalyzed by FKBP12 with inhibition constants ($K_{i,app}$) as low as 1 nM, yet they possess remarkable structural simplicity relative to FK506 and rapamycin, from which they are conceptually derived. The atomic structures of three FKBP12-ligand complexes and of one unbound ligand were determined by X-ray crystallography and are compared to the FKBP12-FK506 and FKBP12-rapamycin complexes.

Introduction

The immunosuppressants FK506¹ and rapamycin² (Figure 1) are structurally related microbial products which block T-cell activation and proliferation.³⁻⁶ The discovery that FK506 and rapamycin each bind with high affinity to the immunophilin FKBP (FK506 binding protein),⁷⁻⁹ a cytosolic enzyme which catalyzes the *cis-trans* isomerization (rotamerization) of prolyl amide bonds,¹⁰ supported the view that inhibition of rotamase activity was responsible for disrupting essential T-cell activation events. This notion originated with the earlier discovery that cyclophilin (cyclosporin binding protein, CyP) is a rotamase, which is unrelated to FKBP, and is selectively inhibited by the potent immunosuppressant cyclosporin A (CsA).^{11,12} Surprisingly, FK506 and rapamycin were found to block different T-cell cytoplasmic signal transduction pathways^{3,5,13,14,18}—an observation inconsistent with a simple enzyme inhibitor mechanism of

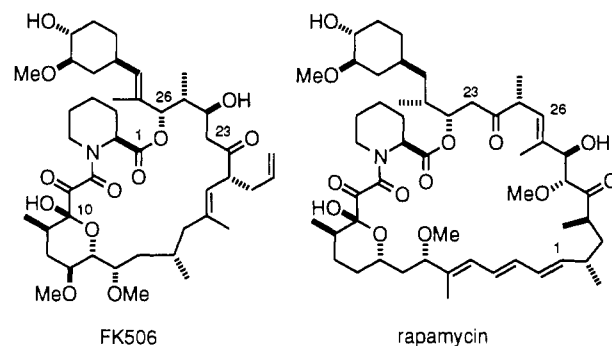


Figure 1. Natural product FKBP ligands.

drug action. FK506 (like CsA) disrupts early T-cell activation events, such as IL-2 secretion, which result from stimulation of the T-cell receptor and are associated with an immediate rise in cytoplasmic Ca^{2+} concentrations.¹⁴⁻¹⁷ Rapamycin, on the other hand, has no effect on IL-2 production but rather interrupts later events associated with signal from the lymphokine receptor.⁶ Additionally, FK506 and rapamycin act as reciprocal antagonists to each other, implying the existence of a common multifunctional receptor.¹⁸ In a landmark study, Schreiber and co-workers¹⁹ prepared a non-immunosuppressive FKBP ligand (506BD) and definitively demonstrated that the inhibition of rotamase activity alone cannot account for the biological activity of these anti-proliferative agents, even though FKBP appears to play an essential role. Complementing the studies in mammalian cells, it was demonstrated that deletion of the gene encoding the predominant FKBP in rapamycin-sensitive yeast produced viable

[†] Department of Medicinal Chemistry, SmithKline Beecham Pharmaceuticals.

[‡] Department of Physical & Structural Chemistry, SmithKline Beecham Pharmaceuticals.

[§] Department of Chemistry, Cornell University.

* Abstract published in *Advance ACS Abstracts*, October 1, 1993.

(1) Tanaka, H.; Kuroda, A.; Marusawa, H.; Hatanaka, H.; Kino, T.; Goto, T.; Hashimoto, M.; Taga, T. *J. Am. Chem. Soc.* **1987**, *109*, 5031-5033.

(2) Swindells, D. C. N.; White, P. S.; Findlay, J. A. *Can. J. Chem.* **1978**, *56*, 2491-2492.

(3) Change, J. Y.; Sehgal, S. N.; Bansbach, C. C. *Trends Pharmacol. Sci.* **1991**, *12*, 218-223.

(4) Kino, T.; Hatanaka, H.; Miyata, S.; Inamura, N.; Nishiyama, M.; Yajima, T.; Goto, T.; Okuhara, M.; Kohsaka, M.; Aoki, H.; Ochiai, T. *J. Antibiot.* **1987**, *9*, 1256-1265.

(5) Morris, R. E. *Immunol. Today* **1991**, *12*, 137-140.

(6) Kay, J. E.; Kromwell, L.; Doe, S. E. A.; Denyer, M. *Immunology* **1991**, *72*, 544-549.

(7) Siekierka, J. J.; Hung, S. H. Y.; Poe, M.; Lin, C. S.; Sigal, N. H. *Nature* **1989**, *341*, 755-757.

(8) Harding, M. W.; Galat, A.; Uehling, D. E.; Schreiber, S. L. *Nature* **1989**, *341*, 758-760.

(9) The family of proteins which bind FK506 and rapamycin have been collectively named FKBP (for FK506 binding proteins). The most abundant member of this family, a 12 kD protein of 107 amino acids originally referred to as FKBP,^{7,8} is more precisely designated as FKBP12. Other higher molecular weight members of this family have also been characterized including FKBP13,^{6,3} FKBP25,^{6,4,6,5} and FKBP59.^{6,6-8}

(10) Harrison, R. K.; Stein, R. L. *J. Am. Chem. Soc.* **1992**, *114*, 3464-3471.

(11) Takahashi, N.; Hayano, T.; Suzuki, M. *Nature* **1989**, *337*, 473-475.

(12) Fischer, G.; Wittman-Liebold, B.; Lang, K.; Kiefhaber, T.; Schmid, F. X. *Nature* **1989**, *337*, 476-478.

(13) Dumont, F. J.; Staruch, M. J.; Koprak, S. L.; Melino, M. R.; Sigal, N. H. *J. Immunol.* **1990**, *144*, 251-258.

(14) Tocci, M. J.; Matkovich, D. A.; Collier, K. A.; Kwok, P.; Dumont, F.; Lin, S.; Degudicibus, S.; Siekierka, J. J.; Chin, J.; Hutchinson, N. I. *J. Immunol.* **1989**, *143*, 718-726.

(15) Kay, J. E.; Benzie, C. R.; Goodier, M. R.; Wick, C. J.; Doe, S. E. A. *Immunology* **1989**, *67*, 473-477.

(16) Bierer, B. E.; Schreiber, S. L.; Burakoff, S. J. *Eur. J. Immunol.* **1991**, *21*, 439-445.

(17) Mattila, P. S.; Ullman, K. S.; Fiering, S.; Emmel, E. A.; McCutcheon, M.; Crabtree, G. R.; Herzenberg, L. A. *EMBO J.* **1990**, *9*, 4425-4433.

(18) Dumont, F. J.; Melino, M. R.; Staruch, M. J.; Koprak, S. L.; Fischer, P. A.; Sigal, N. H. *J. Immunol.* **1990**, *144*, 1418-1424.

(19) Bierer, B. E.; Somers, P. K.; Wandless, T. J.; Burakoff, S. J.; Schreiber, S. L. *Science* **1990**, *250*, 556-559.

organisms that were insensitive to rapamycin,²⁰ implying that the biological actions of FK506 and rapamycin are mediated through FKBP via a gain of function of the protein–drug complex, not through a loss of rotamase catalytic activity.

Thus, the FKBP–FK506 and FKBP–rapamycin complexes apparently function as the modulators of signal transduction, each complex having a distinct biological mechanism, by interacting with distinct downstream targets associated with calcium-dependent and calcium-independent pathways, respectively.^{21–23} In fact, the FKBP12–FK506 complex (and the CyP–CsA complex) has recently been shown to directly inhibit calcineurin, a calcium-dependent protein phosphatase (PP2B), both *in vitro*²⁴ and *in vivo*.²⁵ The inhibition of calcineurin has been postulated to block the translocation of the cytosolic component of NF-AT (nuclear factor of activated T-cells) into the nucleus, resulting in the disruption of IL-2 gene transcription.²⁶ On the other hand, the target protein of the FKBP–rapamycin complex (which does not inhibit calcineurin) is unknown. Several laboratories have recently reported on the inhibition of the activation of the p70 S6 kinase by rapamycin; however, the molecular details of the signaling pathway leading to the activation of this kinase are as yet unresolved as is the precise biomolecular site of intervention by rapamycin.^{27–30}

It has been suggested, and supported by biochemical and structural studies, that FK506 and rapamycin possess two functional molecular domains, a common FKBP-binding domain and dissimilar effector domains. The totally synthetic molecule, 506BD, which possesses the binding domain of FK506 (and rapamycin) and a non-natural replacement for the effector domain, binds to and inhibits FKBP rotamase activity but is not immunosuppressive—consistent with a dual domain model for drug action.¹⁹ Indeed, X-ray crystallographic structure determinations of the FK506 and rapamycin complexes with FKBP12 have revealed that the common domains of the natural products bind in a nearly identical fashion within a hydrophobic pocket of FKBP12 and that the dissimilar effector domains protrude from the protein forming unique protein–drug composite surfaces.^{31,32} These composite surfaces are proposed to constitute the sites of interaction with the downstream target proteins. This model is supported by reports that specific modifications to either the FK506 effector domain³³ or to FKBP12 residues proximal to the FK506 binding site^{34,35} can affect both the calcineurin inhibition by the complex *in vitro* as well as the potency of the modified drugs in cellular assays without significantly influencing the binding of drug to the immunophilin.

(20) Koltin, Y.; Faucette, L.; Bergsma, D. J.; Levy, M.; Cafferkey, R.; Koser, P. L.; Johnson, R. K.; Livi, G. P. *Mol. Cell. Biol.* **1991**, *11*, 1718–1723.

(21) Schreiber, S. L. *Science* **1991**, *251*, 283–287.

(22) Schreiber, S. L.; Liu, J.; Albers, M. W.; Rosen, M. K.; Standaert, R. F.; Wandless, T. J.; Somers, P. K. *Tetrahedron* **1992**, *48*, 2545–2558.

(23) Rosen, M. K.; Schreiber, S. L. *Angew. Chem., Int. Ed. Engl.* **1992**, *31*, 384–400.

(24) Liu, J.; Farmer, J. D., Jr.; Lane, W. S.; Friedman, J.; Weissman, I.; Schreiber, S. L. *Cell* **1991**, *66*, 807–815.

(25) Fruman, D. A.; Klee, C. B.; Bierer, B. E.; Burakoff, S. J. *Proc. Natl. Acad. Sci. U.S.A.* **1992**, *89*, 3686–3690.

(26) Flanagan, W. M.; Corthesy, B.; Bram, R. J.; Crabtree, G. R. *Nature* **1991**, *352*, 803–807.

(27) Kuo, C. J.; Chung, J.; Florentino, D. F.; Flanagan, W. M.; Blenis, J.; Crabtree, G. R. *Nature* **1992**, *358*, 70–73.

(28) Price, D. J.; Grove, R.; Calvo, V.; Avruch, J.; Bierer, B. E. *Science* **1992**, *257*, 973–977.

(29) Calvo, V.; Crews, C. M.; Vik, T. A.; Bierer, B. E. *Proc. Natl. Acad. Sci. U.S.A.* **1992**, *89*, 7571–7575.

(30) Schreiber, S. L. *Cell* **1992**, *70*, 365–368.

(31) Van Duyne, G. D.; Standaert, R. F.; Karplus, P. A.; Schreiber, S. L.; Clardy, J. *Science* **1991**, *252*, 839–842.

(32) Van Duyne, G. D.; Standaert, R. F.; Schreiber, S. L.; Clardy, J. *J. Am. Chem. Soc.* **1991**, *113*, 7433–7434.

(33) Liu, J.; Albers, M. W.; Wandless, T. J.; Luan, S.; Alberg, D. G.; Belshaw, P. J.; Cohen, P.; MacKintosh, C.; Klee, C. B.; Schreiber, S. L. *Biochemistry* **1992**, *31*, 3896–3901.

(34) Aldape, R. A.; Futer, O.; DeCenzo, M. T.; Jarrett, B. P.; Murcko, M. A.; Livingston, D. J. *J. Biol. Chem.* **1992**, *267*, 16029–16032.

(35) Yang, D.; Rosen, M. K.; Schreiber, S. L. *J. Am. Chem. Soc.* **1993**, *115*, 819–820.

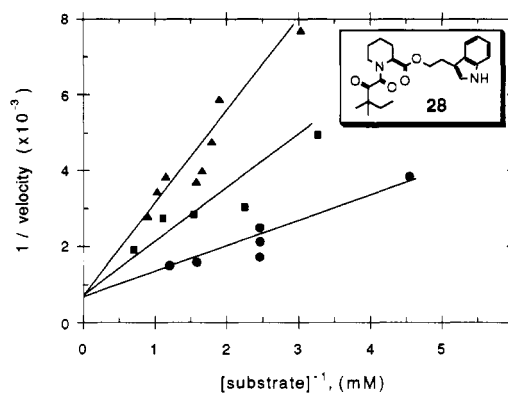


Figure 2. Plot showing the competitive inhibition of FKBP12 catalytic activity by compound **28**. The rotamase activity of FKBP12 was determined using the modified chymotrypsin-coupled assay³⁶ in the presence of varying concentrations of both peptide substrate (succinyl-Ala-Leu-Pro-Phe-4-nitroanilide) and inhibitor. Concentrations of compound **28** employed were 0 (●), 350 (■), and 700 (▲) nM. Data was best fit to a competitive inhibition pattern using the Cleland program⁶⁰ with $K_m = 0.8 \pm 0.4$ mM, $k_{cat} = 1400$ s⁻¹, and $K_i = 220 \pm 50$ nM. For comparison, the apparent inhibition constant ($K_{i,app}$) for compound **28** determined by Dixon analysis⁵⁶ using the standard assay protocol was determined to be 330 ± 50 nM.

As part of a program to discover novel immunosuppressive agents we set out to synthesize compounds that could mimic the biological actions of FK506 and/or rapamycin in disrupting T-cell function but with significantly reduced molecular complexity. Central to the design strategy was the recognition and exploitation of the dual domain (binding and effector) nature of the natural immunosuppressants. A two-phase approach was envisioned beginning with the identification of simplified binding domains which could subsequently be equipped with suitable effector motifs. Thus, our initial goal was to define the factors governing the molecular recognition of FK506 by FKBP and, in the process, identify high-affinity ligands (binding domains) which could serve as synthetic platforms for the attachment of FK506-type or rapamycin-type effector domains.

Results and Discussion

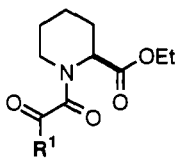
The FK506/rapamycin binding domain is generally viewed to include all of the common structural elements extending from the cyclohexylethyl macrocyclic ring appendage, through the peicolate α -keto amide, and including the pyranose ring.²¹ The X-ray crystal structures of the FK506 and rapamycin complexes with FKBP12, in fact, show these fragments to be the principal contributors to the protein–ligand interface.^{31,32} Thus, initial structure–activity studies were focused on simplifying modifications to the regions of the FK506 binding domain flanking the central peicolyl core, that is, the cyclohexyl and pyranose regions.

As FK506 inhibits FKBP rotamase activity ($K_i \approx 0.4$ nM) commensurately with binding ($K_d \approx 0.4$ nM) and was suggested (though not demonstrated) to be an active site inhibitor,²¹ we have used the inhibition of rotamase activity (expressed throughout as apparent inhibition constants, $K_{i,app}$) as a methodology for the estimation of the relative binding affinities of ligands. During the course of these studies, we have demonstrated competitive inhibition by one of the subject compounds (**28**) against a peptide substrate (Figure 2) as support that the rotamase catalytic site and ligand binding site of FKBP12 are physically coincident. This result provides validation in our use of inhibition constants as a measure of relative ligand binding affinities.³⁶

The entry point for these studies was the examination of variations on the pyranose region in ethyl peicolyl α -keto amides

(36) Both FKBP and CyP have been shown to follow classical Michaelis–Menton kinetics with peptidyl substrates, and competitive inhibition of CyP by a cyclosporin analog has been demonstrated: Kofron, J. L.; Kuzmic, P.; Kishore, V.; Colon-Bomilla, E.; Rich, D. H. *Biochemistry* **1991**, *30*, 6127–6134.

Table I



compd no.	R ¹	K _{i,app} (nM)
1		1600 ± 130
2		2000 ± 300
3		660 ± 60

(Table I).³⁷ Compound **1**, containing a cyclohexyl ring in place of the tetrahydropyran, was found to inhibit FKBP rotamase activity with a $K_{i,app}$ of 1.6 μ M. As seen in the X-ray structure, the hemiketal hydroxyl of FK506 (and rapamycin) is involved in a hydrogen bond to Asp-37 of FKBP.³¹ Furthermore, 10-deshydroxy-FK506 exhibits 50-fold lower affinity than FK506.³⁸ Nevertheless, removal of the hydroxyl from **1**, resulting in **2**, had no detrimental effect on its interaction with FKBP as **2** exhibited comparable inhibitory activity ($K_{i,app} = 2.0 \mu$ M). In fact, replacement of the cyclohexane with bulky alkyl groups leads to slightly higher affinity as observed for the *tert*-pentyl analog **3** ($K_{i,app} = 0.66 \mu$ M).

Mimicry of the FK506 cyclohexylethenyl domain with unsubstituted cyclohexylpropyl and phenylpropyl pipercolyl esters resulted in 3- to 6-fold enhancement of inhibition over the corresponding ethyl ester analogs (Table II, **4** and **5**, $K_{i,app} = 186$ and 110 nM, respectively). Even greater inhibitory potency was seen with substituted aryl analogs such as the 3,4,5-trimethoxyphenyl congener (**6**, $K_{i,app} = 12$ nM). These results are consistent with the observed contribution to binding by the cyclohexylethenyl fragment of 506BD (a factor of approximately 60).³⁹

With an eye toward providing a suitable scaffold for attachment of potential effector elements, substitution at the primary carbinol center was examined. Whereas 1,1-dimethyl-2-propenyl substitution was tolerated with a minor loss in potency (**7**, $K_{i,app} = 250$ nM), phenyl and cyclohexyl substitution resulted in an unanticipated 10-fold increase in affinity ($K_{i,app} = 10$ and 7 nM for **8** and **9**, respectively). Notably, the absolute stereochemistry of the carbinol is critical for both phenyl and cyclohexyl analogs—the *R* epimers exhibiting a 30- to 60-fold greater binding affinity (cf. Table II, **8** vs **10** and **9** vs **11**).

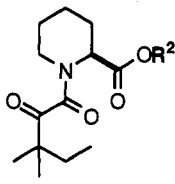
To explore the effects of macrocyclization in simpler systems as well as to provide alternative frameworks for elaboration of effector domains, a series of macrocyclic compounds was synthesized (Table III). Maintaining the pipercolyl 3,3-dimethyl-2-ketobutyramide core (cf. **3**) and also providing a convenient means of convergent analog synthesis, a hydroxylated *tert*-butyl was selected as the pyranose replacement. This allowed for rapid synthetic entry into a wide variety of macrocyclic structures. Simple macrolides bearing no cyclohexylethyl substitution, exemplified by compounds **12** and **13**, exhibited ring-size-dependent inhibition constants in the range of mid nanomolar (30 and 100 nM for **12** and **13**, respectively) to low micromolar (compounds and data not shown).

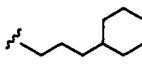
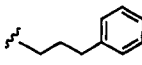
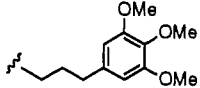
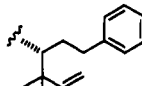
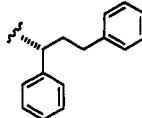
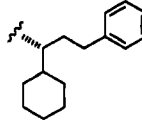
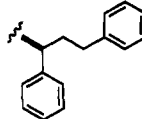
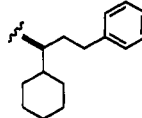
(37) During the preparation of this manuscript a related report on FKBP inhibitors appeared: Hauske, J. R.; Dorff, P.; Julin, S.; DiBrino, J.; Spencer, R.; Williams, R. *J. Med. Chem.* **1992**, *35*, 4284–4296.

(38) Donald, D. K., Fisons Pharmaceuticals, personal communication.

(39) Somers, P. K.; Wandless, T. J.; Schreiber, S. L. *J. Am. Chem. Soc.* **1991**, *113*, 8045–8056.

Table II



compd no.	R ²	K _{i,app} (nM)
4		186 ± 24
5		110 ± 20
6		12 ± 5
7		250 ± 30
8		10 ± 1
9		7 ± 2
10		300 - 600
11		300 ± 40

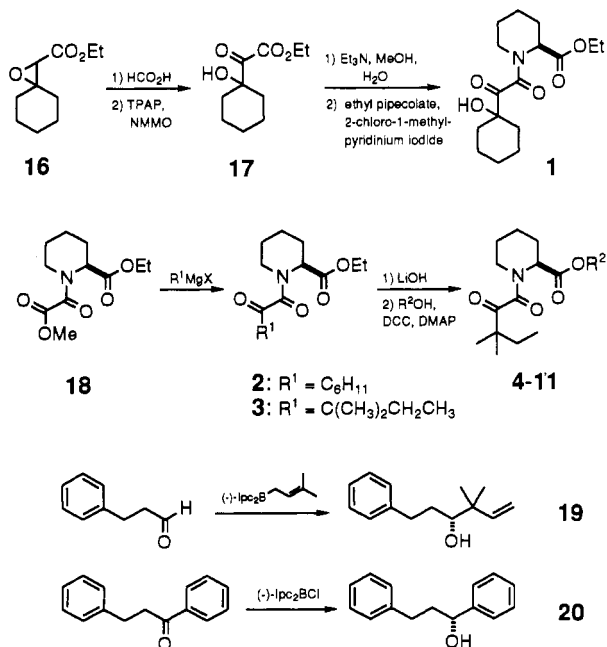
The greatest activity of the compounds examined was observed for members of a bis-macrolide family exemplified by **14** in which the key 1,3-diphenylpropyl subunit of **8** was incorporated in the form of an intramacrocyclic phenylene group and an extramacrocyclic phenethyl substituent. Compound **14** exhibited an FKBP12 apparent inhibitory constant of 1 nM. As was the case for the non-macrocyclic analogs, the potency in this series was also highly dependent on the carbinol stereochemistry—the *S* epimer **15** being over 1000-fold less active.

Synthesis

Compound **1** was prepared in four steps from the Darzen's condensation product, epoxy ester **16** (Scheme I). Notable was the facility of α -keto ester hydrolysis which was effected with triethylamine in methanol and water. The corresponding cyclohexyl and *tert*-pentyl analogs **2** and **3** were prepared by selective addition of the alkyl Grignard reagents to the methyl oxamate **18**. Subsequent basic hydrolysis of the ethyl ester **2** followed by coupling of the appropriate primary or secondary alcohol using dicyclohexylcarbodiimide (DCC) provided the pipercolyl ester analog series **4–11** (Table II). The homoallylic alcohol **19** utilized in the synthesis of *tert*-pentenyl analog **7** was prepared enantiospecifically using the dimethylallylborane methodology of

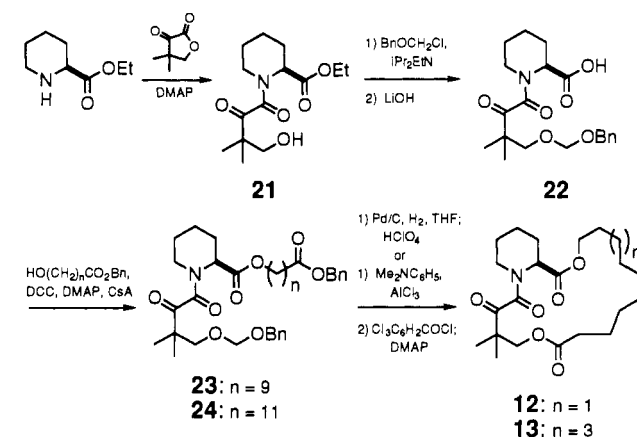
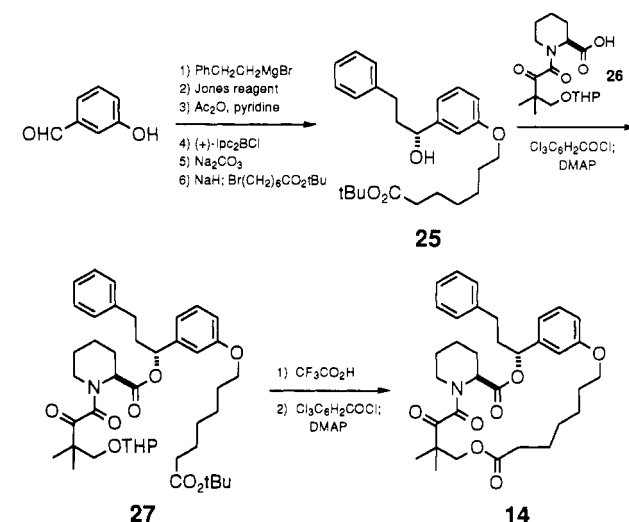
Table III

compd no.	Structure	$K_{i,app}$ (nM)
12		30 ± 10
13		100 ± 20
14		1 ± 0.4
15		>1000

Scheme I

Brown.⁴⁰ Enantiomeric benzyl alcohols **20** and **31** were prepared enantioselectively via a *B*-chlorodiisopinocampheylborane reduction of the ketone; stereochemical assignments of **20** and **31** were based on well-established precedent.⁴¹ Cyclohexyl-substituted analogs **9** and **11** were prepared as a diastereomeric mixture from racemic 3-phenyl-1-cyclohexylpropanol and separated

(40) Brown, H. C.; Jadhav, P. K. *Tetrahedron Lett.* **1984**, *25*, 1215–1218.
 (41) Chandrasekharan, J.; Ramachandran, P. V.; Brown, H. C. *J. Org. Chem.* **1985**, *50*, 5446–5448.

Scheme II**Scheme III**

chromatographically. Assignment of stereochemistry was ultimately confirmed by X-ray crystal structure determination of **9** bound to FKBP12.

Synthesis of the macrocyclic systems (Table III) relied on the intermediacy of **21** which was derived from ethyl pipercolate and dihydro-4,4-dimethyl-2,3-furandione (Scheme II). For **12** and **13**, protection of the primary alcohol of **21** as the BOM ether followed by ester hydrolysis and re-esterification with the appropriate ω -hydroxyalkanoic acid benzyl ester provided the doubly protected macrocyclization precursors **23** and **24**. Following unmasking of the termini, lactonization was accomplished using modified-Yamaguchi conditions.⁴²

Similarly, a convergent strategy was employed for the preparation of **14** and **15** (Scheme III). Optically pure hydroxy ester **25** was prepared in six steps, relying again on a Brown chiral reduction step for installation of the *R*-configured carbinol center. Coupling of **25** to the THP-protected pipercolic acid derivative **26** provided the macrocyclic precursor **27**. Double deprotection followed by Yamaguchi macrocyclization⁴³ provided **14**.

X-ray Crystallographic Structure Analysis

An important contribution to any rational drug design effort can be the knowledge of the 3-dimensional structure of receptors, ligands, or preferably, receptor–ligand complexes. The high-affinity FKBP ligands reported here were designed solely on the basis of a common structural motif presented by three known ligands—FK506, rapamycin, and 506BD—and presumed to

(42) Hikota, M.; Tone, H.; Horita, K.; Yonemitsu, O. *J. Org. Chem.* **1990**, *55*, 7–9.

(43) Inanaga, J.; Katsuki, T.; Takimoto, S.; Ouchida, S.; Inone, K.; Nakano, A.; Okukuda, N.; Yamaguchi, M. *Chem. Lett.* **1979**, 1021–

Table IV. Root-Mean-Square Differences in FKBP12–FK506 Atom Positions vs Complexes with **8**, **9**, and **13**

compd no.	α -carbons	backbone atoms	all atoms
8	0.40	0.41	1.15
9	0.42	0.43	1.09
13-A	0.44	0.45	1.17
13-B	0.51	0.51	1.12

constitute the principal FKBP recognition region (binding domain). As discussed above, subsequent solution of the atomic structures of the FKBP12 complexes with FK506 and rapamycin provided confirmation of the binding domain hypothesis and further illuminated the role of the respective effector domains in shaping unique protein–drug composite pharmacophores. The determinations of X-ray crystal structures for three synthetic ligands (**8**, **9**, and **13**) complexed with FKBP12 were carried out (1) to establish that the binding mode of the synthetic binding domains to FKBP was actually FK506/rapamycin-like, (2) to further elucidate details of the ligand–FKBP interactions guiding the design of improved binding domains, and (3) to provide topographical surveys of the solvent-exposed regions of the docked ligands which are ultimately to serve as platforms for the construction of novel effector domains.

The protein components of all three of the FKBP12–small molecule complexes adopt the same folding topology as found in uncomplexed FKBP12^{44,45} and in complexes of FKBP12 with FK506^{31,46} and rapamycin³²—a five-stranded antiparallel β -sheet wrapping around a short α -helix. No significant main chain conformational differences from the FKBP12–FK506 structure are observed. The root-mean-square (rms) deviations in atom positions between FKBP12–FK506 and the three new FKBP12 complexes are listed in Table IV.

All three synthetic ligands display a binding mode analogous to that of FK506 and rapamycin with the common elements of the piperolate and α -keto amide regions being nearly superimposable in all five structures (Figure 3). The pipercolyl ring of each ligand sits atop the indole of Trp-59, which forms the floor of the FKBP binding pocket. Hydrogen bonds between the amide carbonyl and Tyr-82-OH and between the pipercolyl ester carbonyl and Ile-56-NH are observed in all three structures and are in common with the FK506 and rapamycin complexes. As with FK506 and rapamycin, the synthetic ligands (which exist as mixtures of amide rotamers in solution) bind in a trans amide conformation with the α -keto carbonyl orthogonal to the plane of the amide. Thus, in each case, the ketone oxygen engages the three ϵ -hydrogens of the triad of aromatic residues (Tyr-26, Phe-36, and Phe-99) which form the apparent carbonyl binding pocket of FKBP.

In the FKBP–**8** and FKBP–**9** complexes, the ligands are deeply imbedded in the protein with only about 30% of their surfaces exposed to water. The phenethyl fragments of these nonmacrocyclic inhibitors lie in the same shallow hydrophobic groove of the protein as do the cyclohexyleth(en)yl chains of FK506 and rapamycin, although the aryl rings of **8** and **9** are rotated approximately 90° to the plane of the corresponding cyclohexyl rings of FK506 and rapamycin (Figure 4).⁴⁷ Hydrophobic interactions are made with Tyr-82 and Ile-56 (Figure 5) which account for the approximate 3- to 6-fold increase in affinities observed for analogs bearing longer lipophilic esters (e.g., **3** vs **4** or **5**). The order of magnitude difference in $K_{i,app}$ between **5** and **6** is likely a result of increased hydrophobic interactions of the methoxyl groups of **6** within this shallow groove of the protein

(44) Michnick, S. W.; Rosen, M. K.; Wandless, T. J.; Karplus, M.; Schreiber, S. L. *Science* **1991**, *252*, 836–839.

(45) Moore, J. M.; Peattie, D. A.; Fitzgibbon, M. J.; Thompson, J. A. *Nature* **1991**, *351*, 248–250.

(46) Rotonda, J.; Burbaum, J. J.; Chan, H. K.; Marcy, A. I.; Becker, J. W. *J. Biol. Chem.* **1993**, *268*, 7607–7609.

(47) A similar conformation has been determined by ¹H-NMR for the side chain of a close analog of **8** bound to perdeuterated-FKBP12 in solution; Kumar, V., et al., unpublished results.

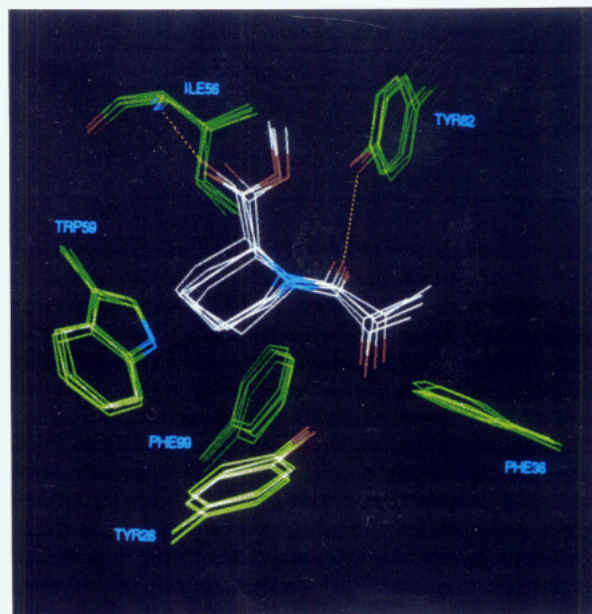


Figure 3. Superimposition of crystal structures of FKBP12 complexed with FK506, rapamycin, **8**, **9**, and **13**. Only partial ligand structures and selected binding pocket residues are shown. Hydrogen bonds are indicated as yellow dashed lines.

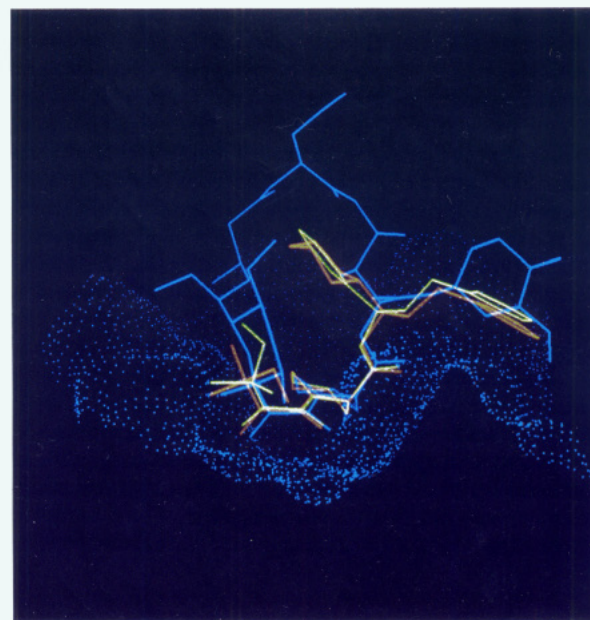


Figure 4. Superimposition of FKBP12–FK506 (blue), FKBP12–**8** (green), and FKBP12–**9** (red) crystal structures showing ligands only. The water-accessible surface for the protein (from the FK506 complex) is shown in part as blue dots.

and suggests a viable structure-based approach to improved inhibitors through optimization of these nonbonded hydrophobic/van der Waals interactions. The 43-hydroxyl cyclohexane substituent of rapamycin (but not the corresponding hydroxyl of FK506) donates a hydrogen bond to the carbonyl of Gln-53. Although the contribution of this particular hydrogen bond to the measured inhibition constant for rapamycin appears to be small, exploitation of such potential hydrogen bond opportunities in second generation inhibitors could also lead to enhancements in binding.

The remaining carbinol substituents of **8** and **9** (phenyl and cyclohexyl, respectively) station themselves more or less over the pipercolyl ring and α -keto amide. Hydrophobic contacts are made with Phe-46 and intramolecularly with the tertiary pentyl groups. The 10- to 15-fold enhancements in binding seen for **8** and **9** over

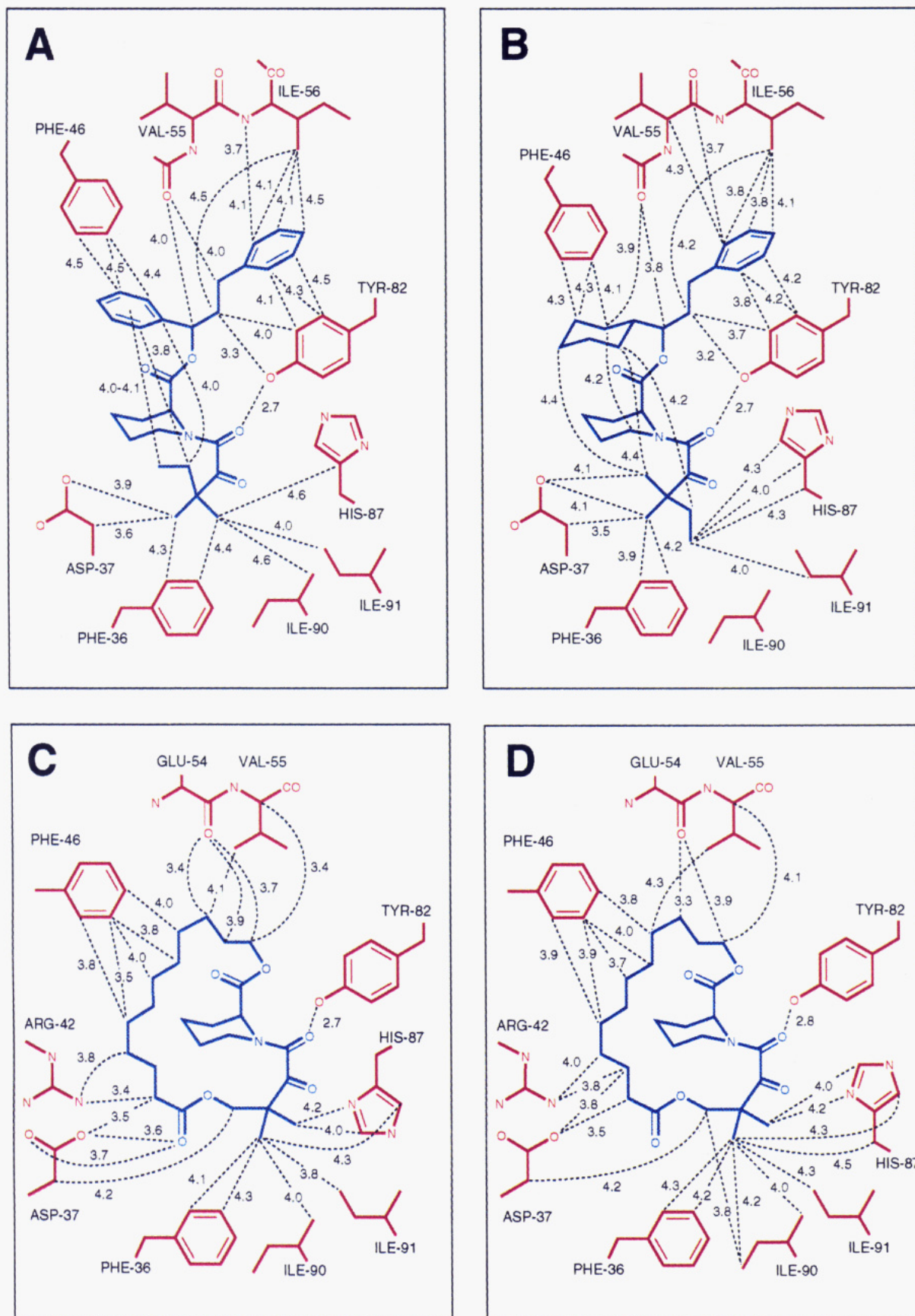


Figure 5. Schematic diagrams indicating selected interatomic distances (in angstroms) for FKBP12 complexes with **8** (panel A), **9** (panel B), and **13** (panels C and D; complexes **13-A** and **13-B**, respectively).

the unsubstituted parent **5** can be explained, in part, by the additional hydrophobic interactions with Phe-46; however, a greater contribution may, in fact, be attributable to intramolecular hydrophobic interactions of the cyclohexyl/phenyl ring between the pipercolyl ring and tertiary pentyl group which effectively

locks the phenethyl group into an optimal binding conformation. This accounts for the different conformation of the tertiary pentyl group in **8** which maximizes this intramolecular interaction with the phenyl substituent centered above the terminal methyl of the 1,1-dimethylpropyl group (Figure 4). This same conformation

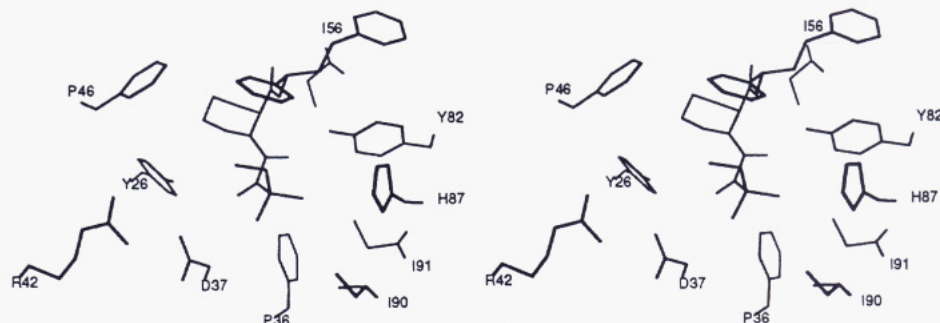


Figure 6. Stereoplot of selected FKBP12 residues which interact with the 1,3-diphenylpropyl ester and tertiary pentyl group of ligand **8**.

of the tertiary pentyl group would result in unfavorable steric interactions with the slightly larger cyclohexyl ring in **9**. The phenyl and cyclohexyl rings of **8** and **9** occupy roughly the same region of the binding pocket as C25–C23 of FK506 and C23–C25 of rapamycin—sections of the natural products near the transition zones between binding and effector domains.²¹ Thus, while modification of these rings might allow for greater protein binding through enhanced hydrophobic interactions or through hydrogen bonding (the C-24 hydroxyl of FK506 and the C-28 hydroxyl of rapamycin both hydrogen bond to the Glu-54 main chain carbonyl, for example), more relevant to drug design is that these six-membered ring appendages may be suitably positioned to serve as foundations for attachment of effector domains.

The lack of increase in affinity observed for **7** (relative to **5**) is consistent with the structural analysis of the FKBP–**9** complex. While the tertiary carbinol substituent of **7** could make similar hydrophobic contacts with the tertiary pentyl group and, to a lesser extent, with Phe-46, proper orientation of the phenethyl side chain would result in an unfavorable A^(1,3) relation between carbons β to the carbinol center. Likewise, compounds **10** and **11**, diastereomers of **8** and **9**, cannot make optimal hydrophobic interactions within the FKBP ligand binding site without adopting unfavorable dihedral angles in the phenethyl side chain.

The tertiary pentyl groups adjacent to the ketone bind in the hydrophobic cavity which also interacts with the pyranose ring of FK506 and rapamycin (Figure 6). With the exception of Asp-37 which is discussed below, the residues which define this pocket (Ile-90, Ile-91, His-87, Phe-36, Tyr-82, and Asp-37) do not move significantly from their positions in the FK506 or rapamycin complexes. Rather, the volume of the tertiary pentyl groups largely fills the same space as the pyranose rings of the natural products, making similar hydrophobic contact with the same binding site residues. For ligand **9**, the five atoms of the tertiary pentyl group overlay very closely five atoms of the FK506 pyranose ring (Figure 4).

The FKBP12–**13** crystals contained two similar but crystallographically distinct complexes in the unit cell (Table IV, **13-A** and **13-B**). The macrocyclic ligands in each of the two complexes adopt binding domain conformations essentially identical with one another as well as with the bound conformations of the non-macrocyclic ligands **8** and **9**. The (CH₂)₁₁ loop of the macrocycle has well-defined electron density and adopts two slightly different conformations in the crystal. The major difference between these conformations is seen in the dodecanoate O=C7–C8–C9 torsion angles (46° and 176° for structures A and B, respectively). Unlike the effector domains of FK506 and rapamycin, which project well out from the FKBP surface (Figure 7), the flexible hydrocarbon chain of **13** loops unobtrusively over the edge of the pipicolate binding pocket formed by Val-55, Phe-46, and the Arg-42/Asp-37 salt bridge (Figure 5). The tertiary butadiyl groups make very similar hydrophobic contacts with the pyranose binding cavity (Phe-36, Ile-90, Ile-91, His-87). The additional lactone functionality, unique to this structure, forms no hydrogen bonds with the protein.

Interestingly, the solid state conformation of unbound **13**, determined by single-crystal X-ray analysis, proved to be

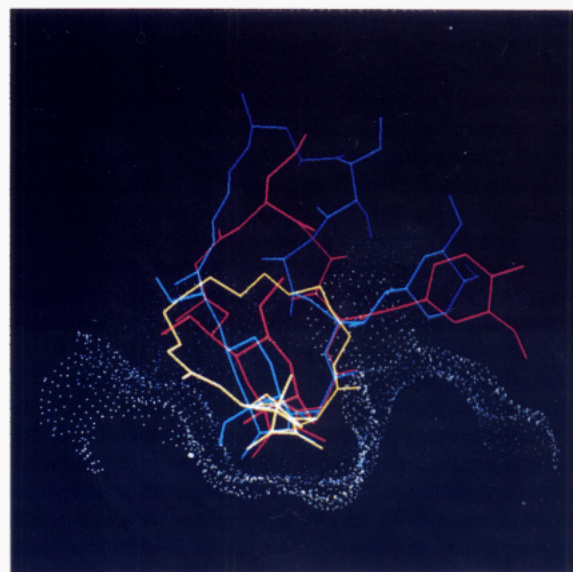


Figure 7. Superimposition of FKBP12–FK506 (red), FKBP12–rapamycin (blue), and FKBP12–**13** (yellow) crystal structures showing ligands only. The water-accessible surface for the protein (from the FKBP12–**13** complex) is shown in part as light blue dots.

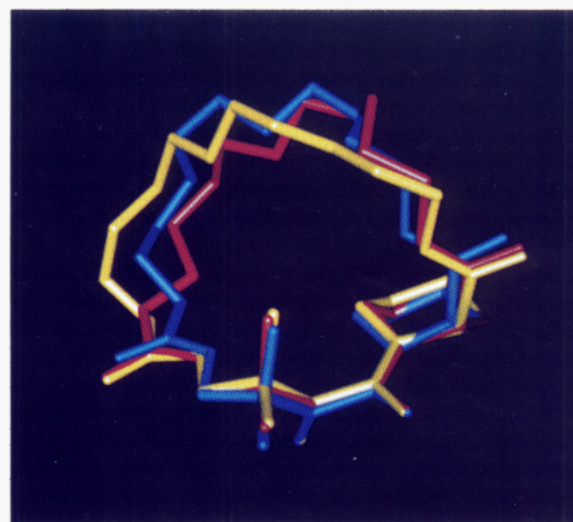


Figure 8. Superimposition of macrocycle **13** crystal structures showing unbound structures as yellow and FKBP12-bound structures as blue (conformer A) and red (conformer B).

superimposable upon both bound conformations of **13** throughout the entire binding domain (Figure 8; rms deviations for 20 atoms, pipicolate oxygens to C1 of dodecanoate, are 0.147 and 0.377). The amide bond is trans and the dicarbonyl torsion angle is 93.5°. The dodecanoate torsion angle (O=C7–C8–C9) is 50.7° and thus similar to the orientation seen in one of the two bound forms. Thus, while macrocycles of this family may be expected to possess

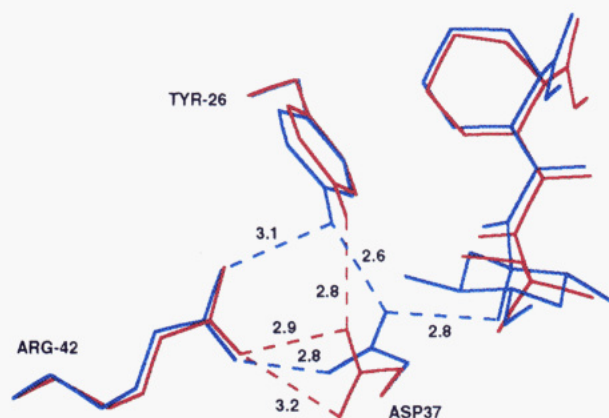


Figure 9. Superimposition of FKBP-FK506 (blue) and FKBP-8 (red) highlighting the change in conformation and hydrogen bonding of Asp-37. Only partial ligand structures are shown. Hydrogen bonds with interatomic distances (in angstroms) are indicated as dashed lines.

considerable conformational mobility, **13** nevertheless appears to have its binding domain significantly preorganized for FKBP complexation.

The exposed ligand binding pocket is flanked by residues 39 to 45 which are referred to as the 40's bulge and residues 77 to 96 which are designated as the 80's loop. Mutagenesis studies suggest that the 80's loop plays an important role in calcineurin binding. For example, the G89P/I90K mutant of FKBP12, while not affecting the binding of FK506, shows dramatic reduction in calcineurin phosphatase inhibition.³⁵ The 80's loop from all three complexes superimposes very well on the corresponding region of the FKBP12/FK506 structure. The rms deviation of all non-hydrogen atoms from residue 79 to residue 96 is 0.54, 0.55, 0.60, and 0.41 Å for the **8**, **9**, **13-A**, and **13-B** complexes, respectively. Even though the average *B*-factor for this region is higher than that of the overall protein, it remains well-defined in the electron density. This observation does not support the idea that the 80's loop can be influenced by inhibitors to adopt different conformations.

The overall conformation of the 40's bulge in these complexes remains the same as that of FKBP12/FK506 as well. The rms deviations of all non-hydrogen atoms in residues 39–45 in **8**, **9**, **13-A**, and **13-B** compared to the FKBP12/FK506 complex are 0.84, 0.92, 1.14, and 1.14 Å respectively. In the FKBP12/FK506 complex, Asp-37 forms a hydrogen bond with the hemiketal hydroxyl of FK506 as well as Arg-42 and Tyr-26. This hydrogen bonding pattern of the Arg-42/Asp-37/Tyr-26 triad is altered in the **8**, **9**, and **13** complexes. Compounds **8**, **9**, and **13** lack the hemiketal hydroxyl present in FK506 and cannot form the hydrogen bond to Asp-37. This results in a consistent shift of the Asp-37 carboxylate away from the inhibitor in all of the complexes, mediated by a minor change (up to 10°) in χ_1 and a larger change in χ_2 of 20 to 30°, which brings the Asp-37 carboxylate into a closer and more coplanar alignment with Arg-42 (Figure 9). In spite of the shift of Asp-37, the overall hydrogen bonding pattern of the salt bridge is maintained and there is little change in the side chains of Arg-42 or Tyr-26 (Figure 9). The **8**, **9**, **13-A**, and **13-B** structures suggest that any further addition to the tertiary pentyl group would have a strong effect on the salt bridge and may even disrupt it completely. Alternatively, if one of the methyl groups of the tertiary pentyl were replaced by a hydroxyl, hydrogen bonding between the ligand and FKBP12 involving Asp-37 should exist and a salt bridge similar to the one in the FK506 complex could be formed. Mutagenesis studies have implicated Arg-42 and Asp-37 as important residues for immunosuppressive activity and indicated that the salt bridge may play an important role in ordering the conformation of residues in this region.^{34,35}

Conclusions

Consideration of the common motif of FK506 and rapamycin as the FKBP-binding domain led to the design and synthesis of highly simplified pipercolate derivatives of both macrocyclic and non-macrocyclic structure which were found to potently inhibit the rotamase activity of FKBP12. The pyranose and oxidized cyclohexylethyl components of the natural product binding domains were effectively supplanted with unfunctionalized aliphatic and phenethyl groups, respectively. X-ray crystallographic analysis of three inhibitor complexes, two non-macrocyclic and one simple macrocycle, with human FKBP12 revealed in each case a binding mode identical with that observed in the crystalline state for both FK506 and rapamycin. The pipercolyl rings, pipercolate esters, and α -keto amides were essentially superimposable in all five structures and displayed similar hydrogen bonding and interaction with the carbonyl binding pocket of the protein. The 3-dimensional structure for the macrocyclic ligand (**13**) in the uncomplexed solid state was determined and proved to be extremely similar to the structure of the bound ligand—suggesting the importance of preorganization in the α -keto amide core of these binding domains.

The relationships between small molecule structures and rotamase inhibitory activities reported here, coupled with atomic resolution pictures of protein–ligand complexes, provide insights into the principles of molecular recognition by the immunophilin FKBP. This understanding should not only lead to the synthesis of FKBP ligands of even greater affinity, but more importantly, it should provide a solid foundation for the design of dual domain ligands bearing the structural elements required to impart biological activities akin to those of FK506 or rapamycin.

Experimental Procedures

General Methods. All reagents and solvents were analytical grade and used as purchased without further purification with the following exceptions: THF was distilled from sodium benzophenone ketyl. Air- and moisture-sensitive reagents were transferred via syringe. All reactions were performed under a positive pressure of argon. ¹H NMR spectra were obtained in CDCl₃ and recorded on Bruker AM-250 (250 MHz) or AM-400 (400 MHz) spectrometers. Chemical shifts are reported in ppm downfield from tetramethylsilane with multiplicity, coupling constants, and integration indicated parenthetically. ¹³C NMR spectra were obtained in CDCl₃ and recorded on a Bruker AM-400 (100.6 MHz) spectrometer and are reported as ppm downfield from tetramethylsilane. Mass spectra (MS), high-resolution mass spectra (HRMS), and elemental analyses were provided by the Analytical and the Physical and Structural Chemistry Departments of SmithKline Beecham Pharmaceuticals. Mass spectral data are reported as the (M + H)⁺ or (M + NH₄)⁺ parent followed by unassigned fragments. Chromatography refers to flash column chromatography using 230–400 mesh silica gel (Merck) and the indicated solvents as the mobile phase. HPLC was conducted using a 4.6 mm × 250 mm Daicel *Chiracel OD* column and (unless otherwise noted) a mobile phase of 95:5 hexane–2-propanol, flow rate of 1 mL/min, and UV detection at 210 nm. Melting points are uncorrected.

Protein Crystallography. Crystallization of the Protein–Ligand Complexes. Recombinant human FKBP12 purified from *Escherichia coli* was obtained at 19.3 mg/mL in 10 mM Tris-HCl pH 8.0 and stored at 4 °C. The drug samples (**8**, **9**, **13**) were dissolved in methanol, mixed in a 3:1 molar ratio with FKBP12 in a vial, and then capped. This solution was lightly vortexed and allowed to sit overnight at 4 °C to ensure complete complex formation. When ready for use, the complex solution was passed through a Millipore 0.22 μ m, low-protein-binding Durapore centrifugation membrane to remove insoluble material, dust, and aggregates. The hanging drop method was used for all crystallizations. Crystals of the **8** or **9** complex were obtained by using HEPES at pHs from 8.5 to 9.0 and Na/K phosphate concentrations of 1.6–1.8 M. The hanging drops were made by mixing 3 μ L of protein–drug complex with 3 μ L of reservoir solution. Large single crystals appeared in 2 or 3 days, growing to a maximum size of 1.0 × 0.80 × 0.25 mm. The crystals were flat plates. Crystals of the **13** complex were obtained from 6 μ L drops consisting of 1.5 μ L of protein–drug complex, 1.5 μ L of water, and 3.0 μ L of well solution of 1.6 M Na/K phosphate at pH 8.0. Crystals grew in 1 to 2 weeks to a size of 0.30 × 0.30 × 0.12 mm and were flat plates with monoclinic morphology.

Table V. Protein Crystallography Data Collection Statistics and Refinement Results

	8	9	13
cell constants			
<i>a</i> (Å)	31.56	31.45	76.31
<i>b</i> (Å)	43.59	43.38	35.03
<i>c</i> (Å)	77.03	77.07	44.38
β (deg)			90.83
space group	<i>P</i> 2 ₁ 2 ₁ 2 ₁	<i>P</i> 2 ₁ 2 ₁ 2 ₁	<i>P</i> 2 ₁
no. of complexes per asymm unit	1	1	2
data collection statistics			
resolution (Å)	25–1.9	25–1.95	25–2.2
no. of reflns meas	20462	18441	18931
no. of unique reflns	8128	6335	11398
<i>R</i> _{sym}	0.114	0.082	0.037
% complete	94	98	94
no. of reflns with <i>F</i> ≥ 2.0 σ	8110	6251	10920
% solvent	44	34	45
no. of refined non-H atoms	954	964	1837
protein	832	832	1664
ligand	33	33	6
solvent	87	132	111
<i>R</i> factor (Å)	0.184 (8–2.0)	0.161 (8–1.95)	0.176 (8–2.2)
final 2 <i>F</i> _o – <i>F</i> _c map (Å)	8.0–2.0	10–1.95	8–2.2
min (e/Å ³)	–3.31	–3.53	–3.26
max	8.85	8.46	7.42
rms	0.945	0.978	0.975
final <i>F</i> _o – <i>F</i> _c (Å)	8–2.0	10–1.95	8–2.2
min	–4.0	–1.187	–6.88
max	4.50	1.341	5.87
rms	0.999	0.997	0.999
rms bond dev (Å)	0.015	0.014	0.011
rms angle dev (deg)	2.99	2.99	2.95
rms improper torsion dev (deg)	2.2	1.2	1.2
av <i>B</i> (all atoms) (Å ²)	9.04	7.5	13.2
av <i>B</i> (ligand) (Å ²)	7.03	13.4	8.7
WA (wt for X-ray term in X-PLOR)	62000	63000	80000

Data Collection. All three data sets were collected on a San Diego multiwire systems area detector with a Rigaku RU-200 copper rotating anode operating at 7.5 kW. Consult Table V for crystallographic details. The space groups for both the 8 and 9 complex are *P*2₁2₁2₁, with very similar cell axes, while the space group for the 13 complex is *P*2₁. All crystals diffracted to moderately high resolution: 1.95, 1.92, and 2.2 Å for the 8, 9, and 13 complexes, respectively. Data were measured at room temperature in 30 s frames of width 0.08° in ω with a crystal-to-detector distance of 356 mm for 8, 30 s frames of width 0.12° in ω with a crystal-to-detector distance of 352 mm for 9, and 30 s frames of width 0.12° in ω with a crystal-to-detector distance of 422 mm for 13. Data reductions were performed on site.⁴⁸ Data collection statistics are given in Table V.

Structure Determination. All three structures were solved by molecular replacement using FKBP12 from either the FKBP12–FK506³¹ or FKBP12–rapamycin³² complex crystal structure as a model.⁴⁹ All calculations were performed using X-PLOR.⁵⁰ Since there was only one molecule per asymmetric unit for the 8 and 9 complexes, cross rotation searches were directly applied using data from 15 to 4.0 Å, and each yielded a single high peak. Patterson correlation refinement suggested that each was the correct orientation. Translation search basing on this orientation give an unambiguous translation solution with an *R* factor of 40% at 15–4.0 Å. Not surprisingly, the rotation and translation solutions for the 8 and 9 complexes were identical. Rigid body refinement at 10–3.0 Å dropped the *R* factor to 35%. The 13 complex contained two molecules per asymmetric unit and a self rotation search using 15–4.0 Å data revealed the presence of a noncrystallographic 2-fold relating the two complexes. The cross rotation search using the FKBP12–FK506 model followed by Patterson correlation refinement gave two unambiguous solutions. The translation solution for the first rotation peak was easily determined using a 1 Å search grid. The noncrystallographic symmetry from the self-rotation search was applied and the second translation solved. The correct orientation of the two molecules with respect to the same

origin was determined and then rigid body refinement carried out to 3.0 Å yielded an *R* factor of 35.0%.

Structure Refinement. Cycles of simulated annealing, conventional positional refinement, and thermal parameter refinement using X-PLOR⁵⁰ followed by manual adjustment using the graphics program Chain⁵¹ were used to refine each of the complexes. In all cases, the drug was clearly defined in a 1 σ difference map computed subsequent to partial protein refinement. Only minor adjustments were required upon further refinement. Water molecules were assigned to 3 σ peaks in the difference map. Only those water molecules with reasonable geometry and *B*-factors lower than 60 Å were accepted. Final refinement results are given in Table V. Coordinates have been deposited with the Brookhaven Protein Data Bank.

X-ray Structure Determination of 13. Crystals of 13 were grown from toluene. A block-shaped specimen of approximate dimensions 0.50 × 0.40 × 0.30 mm was mounted on a glass fiber, coated with Paratone N oil, and flash frozen in a cold stream of nitrogen gas at 223 K. A random search routine led to the unit cell definition which was refined from the setting angles of 25 reflections on an Enraf Nonius CAD4 diffractometer equipped with graphite monochromated molybdenum radiation ($\lambda\alpha = 0.71073$ Å). The space group is *P*2₁/c with *a* = 12.398(2) Å, *b* = 10.063(3) Å, *c* = 19.586(8) Å, $\beta = 96.52(2)^\circ$, *V* = 2427.6(9) Å³, *Z* = 4, $d_{calc} = 1.197$ g/cm³ based on *M_r* = 437.58 for [C₂₄H₃₉NO₆], $\mu = 0.794$ cm⁻¹, *F*(000) = 952. Data were measured on the diffractometer using an ω -2 θ scan mode with a variable scan rate up to 7 deg/min, $2\theta_{max} = 56^\circ$ and index ranges $0 \leq h \leq 16$, $0 \leq k \leq 13$, $-25 \leq l \leq 25$. Intensities were corrected for Lorentz and polarization effects. A unique set of data (5842) were obtained by averaging (*R*_{int} = 0.029).

The structure was solved with SHELXS.⁵² Non-hydrogen atoms were refined with anisotropic displacement parameters. Positions for all of the hydrogen atoms were suggested from difference Fourier maps and these were included as fixed contributions in the final model with assigned isotropic temperature factors. The function minimized in least squares was $\sum w(|F_o| - |F_c|)^2$ with the weights, *w*, defined as $4F_o^2/\sigma(F_o^2)$ and $\sigma(F_o^2) = [\sigma^2(I_c) + (0.0016I_c)]$. Convergence (max $\Delta/\sigma = 0.07$) was reached straightforwardly to final crystallographic residuals of *R* = 0.053, *wR* = 0.058, GOF = 1.452 for a refinement of 280 variables with 1673

(48) Howard, A.; Nielson, C.; Xuong, Ng. H. In *Methods in Enzymology*; Wycoff, H., Hirs, C., Timasheff, S., Eds.; Academic Press: Orlando, 1985; Vol. 114, pp 452–472.

(49) Van Duyne, G.; Standaert, R.; Karplus, P.; Schreiber, S.; Clardy, J. *J. Mol. Biol.* 1993, 229, 105–124.

(50) Brunger, A.; Krukowski, A.; Erikson, J. *Acta Crystallogr.* 1990, A46, 585–593.

(51) Sack, J. *J. Mol. Graphics* 1988, 6, 224–225.

(52) *International Tables for X-ray Crystallography*; Birmingham: Kynoch Press (Present Distributor D. Reidel: Dordrecht), 1974; Vol. IV.

observations. Maximum excursions in a final difference Fourier map were within $\pm 0.203 \text{ e}/\text{A}^3$. Neutral atom scattering factors from the International Tables for X-ray Crystallography⁵³ were used.

Enzyme Assays. PPIase Activity and Inhibition Studies. Human recombinant FKBP12 expressed in *E. coli* (D. Bergsma et al., unpublished) was purified to apparent homogeneity by a procedure similar to that described by Standaert et al.⁵⁴ but modified to eliminate the heat step. The PPIase activity (k_{cat}/K_m) catalyzed by recombinant human FKBP12 was determined using the synthetic peptide succinyl-Ala-Phe-Pro-Phe-4-nitroanilide as substrate in the chymotrypsin-coupled reaction as described for the cyclophilins.⁵⁵ This particular peptide sequence was chosen for use in the analysis of potential inhibitors with FKBP12 since it had the combined characteristics of relatively high catalytic efficiency ($2.2 \text{ s}^{-1}\mu\text{M}^{-1}$), low spontaneous rate of *cis* to *trans* isomerization ($4.3 \times 10^{-3} \text{ s}^{-1}$), and high percentage (21–23%) of *cis* rotamer in solution. Except as noted, assays were performed in 1 mL at 10 °C in 35 mM HEPES, pH 7.8, with 25 μM substrate and monitored at 390 nM with Perkin-Elmer Lambda 4C or Lambda 6 spectrophotometers; assays were initiated by addition of α -chymotrypsin ($\geq 250 \mu\text{g}$) and followed for 5–10 min. Absorbance as a function of time from individual PPIase assays was analyzed by a first-order exponential function corresponding to the *cis* to *trans* isomerization of peptide substrate as previously outlined.⁵⁵ The net-rate constants were normalized to protein concentration as determined by total amino acid content.

In experiments to determine inhibition by FK506, rapamycin, and synthetic molecules, a solution of the test compound in ethanol was added to the incubation mixture prior to initiation of the reaction. The percentage of ethanol in the reactions was constant at 0.5% of the final reaction volume, an amount shown to have minimal effect on FKBP12 PPIase activities. Inhibition of enzymatic activity was determined by Dixon analysis⁵⁶ or using eq 1 describing a reversible tight-binding inhibitor:⁵⁷

$$v_i = (v_o/2E_i) \{ [(K_{i,\text{app}} + I_t - E_t)^2 + 4K_{i,\text{app}}E_t]^{0.5} - (K_{i,\text{app}} + I_t - E_t) \} \quad (1)$$

where v_i and v_o are the enzymatic rates in the presence and absence respectively of inhibitor, I_t and E_t are the total concentrations of inhibitor and enzyme, and $K_{i,\text{app}}$ is the apparent equilibrium inhibition constant. Data were analyzed with eq 1 when the estimated value for the $K_{i,\text{app}}$ approximated or was less than the concentration of FKBP12, typically 28–30 nM, in the individual experiment. Fitting of data to eq 1 was accomplished with a nonlinear regression procedure using the Marquardt algorithm⁵⁸ in the SAS statistical analysis software package (SAS Institute, Inc., Cary, NC). Using this protocol, apparent inhibition constants ($K_{i,\text{app}}$) of 0.3–0.6 and 0.8–2.0 nM were obtained for rapamycin and FK506, respectively; the value for FK506 is in agreement with that reported previously (1.7 nM) using the alternative substrate succinyl-Ala-Leu-Pro-Phe-4-nitroanilide.⁵⁹

Steady-state inhibition analysis of FKBP12 with compound **28** was conducted using modifications to the standard chymotrypsin coupled assay described by Kofron et al.³⁶ in the presence of varying concentrations of inhibitor. Peptide substrate succinyl-Ala-Leu-Pro-Phe-4-nitroanilide, chosen for its improved solubility, was dissolved in anhydrous trifluoroethanol (TFE) containing 400 mM LiCl to enhance the proportion of *cis* isomer. Assays were initiated by addition of substrate in TFE to a solution containing all other assay components pre-equilibrated to 0 °C, the temperature at which the assays were conducted. TFE and ethanol concentrations were kept constant at 2.5% and 0.5%, respectively. True substrate concentrations at each data point and initial reaction velocities were calculated from the initial linear portion of individual progress curves. Initial reaction velocities also were determined by fitting the enzymatic progress curves to the integrated rate equation as described³⁶ using the KineTic program obtained from BioKin Ltd. (Madison, Wisconsin). The two procedures for determining the initial velocities gave comparable

(53) Sheldrick, G. M. In *Crystallographic Computing 3*; Sheldrick, G. M., Kruger, C., Goddard, R., Eds.; Oxford University Press: London, 1985; pp 175–189.

(54) Standaert, R. F.; Galet, A.; Verdine, G. L.; Schreiber, S. L. *Nature* **1990**, *346*, 671–674.

(55) Bergsma, D. J.; Eder, C.; Gross, M.; Kersten, H.; Sylvester, D.; Appelbaum, E.; Cusimano, D.; Livi, G. P.; McLaughlin, M. M.; Kasyan, K.; Porter, T. G.; Silverman, C.; Dunnington, D.; Hand, A.; Pritchett, W. P.; Bossard, M. J.; Brandt, M.; Levy, M. A. *J. Biol. Chem.* **1991**, *34*, 23204–23214.

(56) Dixon, M. *Biochem. J.* **1953**, *55*, 170–171.

(57) Morrison, J. F.; Stone, S. R. *Comments Mol. Cell. Biophys.* **1985**, *2*, 347–368.

(58) Marquardt, D. W. *J. Soc. Ind. Appl. Math.* **1963**, *11*, 431–441.

(59) Harrison, R. K.; Stein, R. L. *Biochemistry* **1990**, *29*, 3813–3816.

results. The combined initial velocity data set with inhibitor **28** was analyzed by the COMP and NONCOMP programs described by Cleland,⁶⁰ best fit of the data to the COMP program was determined by established criteria.⁶⁰

Ethyl 1-Hydroxy- α -hydroxycyclohexanecetate (29). Ethyl β,β -pentamethyleneglycidate (**16**)⁶¹ (500 mg, 2.71 mmol) was dissolved in formic acid (10 mL) and cooled in an ice–water bath at 5 °C. After 20 min, the lightly colored solution was diluted with 250 mL of ethyl acetate, washed with saturated aqueous sodium bicarbonate ($3 \times 75 \text{ mL}$) and brine (50 mL), and concentrated. The residual oil was then dissolved in absolute ethanol (10 mL), cooled in an ice bath, treated with solid potassium carbonate (200 mg, 1.45 mmol), and stirred for 30 min. The reaction mixture was filtered to remove residual solid, and the filtrate was concentrated. Flash chromatography on silica gel (1:3 ethyl acetate–hexane) gave the desired dihydroxy ester **29** (230 mg, 42%) as a colorless oil: ¹H NMR (CDCl₃, 400 MHz) δ 4.28 (dq, $J = 7.2, 1.5 \text{ Hz}$, 2 H), 3.96 (d, $J = 6.7 \text{ Hz}$, 1 H), 3.34 (d, $J = 7.5 \text{ Hz}$, 1 H), 2.47 (s, 1 H), 1.20–1.63 (m, 10 H), 1.33 (t, $J = 7.2 \text{ Hz}$, 3H); ¹³C NMR (CDCl₃, 100.6 MHz) δ 173.2, 73.0, 61.7, 33.5, 33.2, 25.6, 21.5, 21.4, 14.2; IR (film) 3600–3200 (OH), 2930, 2860, 1730, 1450, 1360, 1255, 1200, 1100, 980 cm⁻¹; MS (DCI/NH₃), m/z 220 (M + NH₄)⁺.

Ethyl 1-Hydroxy- α -oxocyclohexanecetate (17). Dihydroxy ester **29** (120 mg, 0.582 mmol) was dissolved in CH₂Cl₂ (2.0 mL) at room temperature under an argon atmosphere. Molecular sieves (4 Å, 250 mg), tetrapropylammonium perruthenate (30.0 mg, 0.0854 mmol), and 4-methylmorpholine N-oxide (126 mg, 1.08 mmol) were added. After 20 min, the thick, black reaction mixture was filtered through a short bed of silica gel, which was washed with 1:1 ethyl acetate–hexane. Concentration of the filtrate yielded the keto ester **17** (60 mg, 48%) as a colorless oil: ¹H NMR (CDCl₃, 400 MHz) δ 4.35 (q, $J = 7.2 \text{ Hz}$, 2 H), 2.82 (s, 1 H), 1.61–1.89 (m, 9 H), 1.38 (t, $J = 7.2 \text{ Hz}$, 3 H), 1.25–1.35 (m, 1 H); ¹³C NMR (CDCl₃, 100.6 MHz) δ 210.0, 163.1, 62.4, 33.4, 25.0, 20.7, 14.0.

(S)-Ethyl 1-[2-(1-Hydroxycyclohexyl)-1,2-dioxoethyl]-2-piperidine-carboxylate (1). A solution of keto ester **17** (20.0 mg, 0.100 mmol), methanol (0.2 mL), water (0.1 mL), and triethylamine (0.075 mL) was stirred for 6 h at room temperature. The reaction mixture was then concentrated and dried in vacuo (24 h, 0.50 mmHg, 25 °C). The resulting triethylammonium salt was then dissolved in 0.500 mL of dichloromethane and ethyl 2(S)-piperidinecarboxylate (20.0 mg, 0.127 mmol), triethylamine (50 mL, 0.36 mmol), and 2-chloro-*N*-methylpyridinium iodide (32.0 mg, 0.125 mmol) were added. After 3 h, the yellow suspension was added directly to a flash chromatography column containing silica gel. Elution with 25% ethyl acetate/hexane afforded the desired amide **1** (14.3 mg, 46%), as a colorless oil: ¹H NMR (CDCl₃, 400 MHz, 3:1 mixture of *trans*–*cis* amide rotamers, data for *trans* amide) δ 5.23 (d, $J = 5.7 \text{ Hz}$, 1 H), 4.23 (q, $J = 7.5 \text{ Hz}$, 2 H), 3.44 (bd, $J = 13.4 \text{ Hz}$, 1 H), 3.28 (td, $J = 13.0, 3.3 \text{ Hz}$, 1 H), 2.83 (s, 1 H), 2.33 (br d, $J = 12.3, 1 \text{ Hz}$), 1.93–1.33 (m, 15 H), 1.30 (t, $J = 7.1 \text{ Hz}$, 3 H); ¹³C NMR (CDCl₃, 100.6 MHz, 3:1 mixture of *trans*–*cis* amide rotamers, data for *trans* amide): δ 209.9, 170.0, 167.5, 62.7, 51.8, 44.7, 34.5, 34.2, 26.6, 25.0, 21.8, 21.0, 14.1; IR (film) 3600–3200 (OH), 2930, 2860, 1740, 1710, 1640, 1440, 1200, 1160, 1140, 1020, 980; MS (DCI/NH₃), m/z 312.3 (M + H)⁺. Anal. Calcd for C₁₆H₂₅NO₅: C, 61.72; H, 8.09; N, 4.50. Found: C, 61.14; H, 7.96; N, 5.07.

Ethyl (2S)-1-(1,2-Dioxo-2-cyclohexylethyl)-2-piperidinecarboxylate (2). A solution of ethyl (2S)-1-(1,2-dioxo-2-methoxyethyl)-2-piperidinecarboxylate (6.06 g, 25.0 mmol) in dry THF (121 mL) was cooled to –78 °C. Cyclohexylmagnesium chloride (12 mL of a 2.0 M ether solution, 24.0 mmol) was added dropwise and the mixture was stirred for 2.5 h at –78 °C. The reaction was quenched at –78 °C with a small amount of ethyl acetate, and then partitioned between ethyl acetate and water, washed with brine, and dried over anhydrous magnesium sulfate. The resulting crude material was purified by silica gel flash chromatography (eluted with gradient 5% to 25% ethyl acetate in hexane) to afford **2** (3.0 g, 40%; 63% based on recovered starting material) along with 2.15 g of recovered starting material: [α]_D²⁵ –57.5° (c 1.04, EtOH); ¹H NMR (CDCl₃, 400 MHz, 3:1 mixture of *trans*–*cis* amide rotamers, data for *trans* rotamer) δ 5.25 (d, $J = 5.6 \text{ Hz}$, 1 H), 4.23 (q, $J = 7.2 \text{ Hz}$, 2 H), 3.56 (d, $J = 13.1 \text{ Hz}$, 1 H), 3.21 (td, $J = 13.1, 3.2 \text{ Hz}$, 1 H), 2.95–2.86 (m, 1 H), 2.33 (br d, $J = 13.0 \text{ Hz}$, 1 H), 1.30 (t, $J = 7.2 \text{ Hz}$, 3H); IR (neat) 2945, 1745, 1715, 1650, 1450, 1210, 1025 cm⁻¹; MS

(60) Cleland, W. W. *Methods Enzymol.* **1979**, *63*, 103–138.

(61) Hunt, R. H.; Chinn, L. J.; Johnson, W. S. In *Organic Synthesis*; Rabjohn, N., Ed.; John Wiley & Sons, Inc.: New York, 1963; Collect. Vol. IV, pp 459–460.

(DCI/NH₃), *m/z* 313 (M + NH₄)⁺, 296. Anal. Calcd for C₁₆H₂₅NO₄: C, 65.06; H, 8.53; N, 4.74. Found: C, 64.71; H, 8.27; N, 4.60.

Ethyl (2S)-1-(1,2-Dioxo-3,3-dimethylpentyl)-2-piperidinecarboxylate (3). To a solution of methyl (2S)-1-(1,2-dioxo-2-methoxyethyl)-2-piperidinecarboxylate (3.65 g, 15.0 mmol) in THF (30 mL) at -78 °C was added 1,1-dimethylpropylmagnesium chloride (20 mL of a 1.0 M ether solution, 20 mmol) under an argon atmosphere and the reaction mixture was stirred for 3 h at -78 °C. The reaction mixture was then poured into saturated aqueous NH₄Cl and extracted with ethyl acetate. The organic extract was washed with brine, dried over anhydrous magnesium sulfate, and concentrated. Chromatography (5% ethyl acetate in hexane) afforded **3** (3.1 g, 73%) as a colorless oil: ¹H NMR (CDCl₃, 250 MHz, 4:1 mixture of trans-cis amide rotamers, data for trans rotamer) δ 5.25 (d, *J* = 6.6 Hz, 1 H), 4.23 (q, *J* = 7.1 Hz, 2 H), 3.4 (br d, *J* = 13 Hz, 1 H), 3.2 (td, *J* = 13.0, 3 Hz, 1 H), 2.35 (br d, *J* = 13 Hz, 1 H), 1.80–1.35 (m, 7 H), 1.29 (t, *J* = 7.1 Hz, 3 H), 1.25 (s, 3 H), 1.21 (s, 3 H), 0.9 (t, *J* = 7.4 Hz, 3 H); IR (neat) 1745, 1710, 1650, 1445, 1205, 1025 cm⁻¹; MS (DCI/NH₃), *m/z* 301 (M + NH₄)⁺, 284 (M + H)⁺, 158, 84. Anal. Calcd for C₁₅H₂₅NO₄: C, 63.58; H, 8.89; N, 4.94. Found: C, 63.24; H, 8.75; N, 4.97.

(2S)-1-(1,2-Dioxo-3,3-dimethylpentyl)-2-piperidinecarboxylic Acid (30). A mixture of ethyl (2S)-1-(1,2-dioxo-3,3-dimethylpentyl)-2-piperidinecarboxylate (**3**) (3.1 g, 11 mmol), 1 N LiOH (15 mL), and methanol (90 mL) was stirred at 0 °C for 30 min and then at room temperature for 6 h. The mixture was then acidified with 10% aqueous HCl diluted with water, and extracted with CH₂Cl₂. The organic extract was washed with water and brine, dried, and concentrated to a white solid (2.25 g, 80%) which was used without further purification: mp 138–139 °C (recrystallized from ethyl acetate-hexane); ¹H NMR (CDCl₃, 400 MHz, 5:1 mixture of trans-cis amide rotamers, data for trans rotamer) δ 5.32 (d, *J* = 5.6 Hz, 1 H), 3.41 (br d, *J* = 13.8 Hz, 1 H), 3.24 (br t, *J* = 13, 1 H), 2.35 (br d, *J* = 13 Hz, 1 H), 1.83–1.40 (m, 7 H), 1.23 (s, 3 H), 1.20 (s, 3 H), 0.89 (t, *J* = 7.4 Hz, 3 H); MS (DCI/NH₃), *m/z* 273 (M + NH₄)⁺. Anal. Calcd for C₁₃H₂₁NO₄: C, 61.16; H, 8.29; N, 5.49. Found: C, 61.21; H, 8.33; N, 5.59.

General Procedure for the Esterification of (2S)-1-(1,2-Dioxo-3,3-dimethylpentyl)-2-piperidinecarboxylic Acid. A solution of the appropriate alcohol in CH₂Cl₂ at room temperature was treated with carboxylic acid **30**, followed by 1,3-dicyclohexylcarbodiimide (DCC), 4-(dimethylamino)pyridine (DMAP), and 10-camphorsulfonic acid (CSA) under an argon atmosphere. The resulting bright yellow suspension was allowed to stir overnight. The mixture was then diluted with a small amount of ethyl acetate, filtered, and concentrated, and the residue was subjected to column chromatography on silica gel. Elution with 15–30% ethyl acetate in hexane provided the desired esters.

3-Cyclohexyl-1-propyl (2S)-1-(3,3-Dimethyl-1,2-dioxopentyl)-2-piperidinecarboxylate (4). A solution of 3-cyclohexyl-1-propanol (100 mg, 0.703 mmol) in CH₂Cl₂ (1.0 mL) was treated with **30** (100 mg, 0.392 mmol), DCC (130 mg, 0.630 mmol), DMAP (14.7 mg, 0.120 mmol), and CSA (28.0 mg, 0.121 mmol) to provide **4** (120 mg, 81%) as a light yellow oil: ¹H NMR (CDCl₃, 400 MHz, 6:1 mixture of trans-cis amide rotamers, data for trans rotamer) δ 5.25 (d, *J* = 5.4 Hz, 1 H), 4.17–4.11 (m, 2 H), 3.39 (br d, *J* = 13.3 Hz, 1 H), 3.23 (td, *J* = 13.0, 3.1 Hz, 1 H), 2.31 (br d, *J* = 12.8 Hz, 1 H), 1.25 (s, 3 H), 1.21 (s, 3 H), 0.90 (t, *J* = 7.4 Hz, 3 H); ¹³C NMR (CDCl₃, 100.6 MHz) δ 207.8, 170.4, 167.4, 65.9, 51.2, 46.7, 43.9, 37.2, 33.4, 33.2, 32.5, 26.5, 26.4, 26.2, 25.9, 24.9, 23.6, 22.9, 21.2, 21.0, 8.7; IR (neat) 2920, 2850, 1740, 1700, 1645, 1440, 1200 cm⁻¹; MS (DCI/NH₃), *m/z* 397 (M + NH₄)⁺, 380. Anal. Calcd for C₂₂H₃₇NO₄: C, 69.62; H, 9.83; N, 3.69. Found: C, 69.49; H, 9.71; N, 4.06.

3-Phenyl-1-propyl (2S)-1-(3,3-Dimethyl-1,2-dioxopentyl)-2-piperidinecarboxylate (5). A solution of 3-phenyl-1-propanol (69 mg, 0.509 mmol) in CH₂Cl₂ (1.0 mL) was treated with **30** (100 mg, 0.392 mmol), DCC (129 mg, 0.627 mmol), DMAP (14.4 mg, 0.117 mmol), and CSA (27.3 mg, 0.117 mmol) to provide **5** (100 mg, 68%) as a colorless oil: ¹H NMR (CDCl₃, 400 MHz, 7:1 mixture of trans-cis amide rotamers, data for trans rotamer) δ 7.31–7.17 (m, 5H), 5.28 (d, *J* = 5.3 Hz, 1 H), 4.18 (t, *J* = 6.3 Hz, 2 H), 3.40 (br d, *J* = 12.4 Hz, 1 H), 3.23 (td, *J* = 12.9, 3.1 Hz, 1 H), 2.70 (t, *J* = 7.6 Hz, 2 H), 2.32 (br d, *J* = 13.0 Hz, 1 H), 1.99 (quintet, *J* = 6.8 Hz, 2 H), 1.25 (s, 3 H), 1.21 (s, 3 H), 0.89 (t, *J* = 7.5 Hz, 3 H); MS (DCI/NH₃), *m/z* 391 (M + NH₄)⁺, 374. Anal. Calcd for C₂₂H₃₁NO₄: C, 70.75; H, 8.37; N, 3.75. Found: C, 70.43; H, 8.30; N, 3.58.

3-(3,4,5-Trimethoxyphenyl)-1-propyl (2S)-1-(3,3-Dimethyl-1,2-dioxopentyl)-2-piperidinecarboxylate (6). A solution of 3-(3,4,5-trimethoxyphenyl)-1-propanol (126 mg, 0.588 mmol) in CH₂Cl₂ (1.0 mL) was treated with **30** (100 mg, 0.392 mmol), DCC (129 mg, 0.627 mmol), DMAP (14.4 mg, 0.117 mmol), and CSA (27.3 mg, 0.117 mmol) to

provide **6** (149 mg, 89%) as a colorless oil: ¹H NMR (CDCl₃, 250 MHz, 7:1 mixture of trans-cis amide rotamers, data for trans rotamer) δ 6.41 (s, 2 H), 5.29 (d, *J* = 5.5 Hz, 1 H), 4.19 (t, *J* = 6.6 Hz, 2 H), 3.86 (s, 6 H), 3.83 (s, 3 H), 3.40 (br d, *J* = 13.2 Hz, 1 H), 3.24 (td, *J* = 12.5, 3.1 Hz, 1 H), 2.65 (t, *J* = 7.6 Hz, 2 H), 2.33 (br d, *J* = 14.0 Hz, 1 H), 1.98 (quintet, *J* = 7.0 Hz, 2 H), 1.24 (s, 3 H), 1.21 (s, 3 H), 0.89 (t, *J* = 7.4 Hz, 3 H); MS (ES), *m/z* 486 (M + Na)⁺, 464 (M + H)⁺. Anal. Calcd for C₂₅H₃₇NO₇·0.4H₂O: C, 63.78; H, 8.09; N, 2.98. Found: C, 63.79; H, 8.14; N, 2.89.

(4R)-3,3-Dimethyl-6-phenyl-1-hexen-4-ol (19). To a suspension of (-)-diisopinocampheborane⁶² (1.43 g, 5 mmol) in pentane (8 mL) at -25 °C was added 3-methyl-1,2-butadiene (0.34 g, 5 mmol). The resulting mixture was stirred at -25 °C to -15 °C for 6 h and then cooled to -78 °C. 3-Phenylpropionaldehyde (0.67 g, 5 mmol) was then added, and the reaction mixture was allowed to stir for 12 h at -78 °C and for 48 h at -20 °C. Absolute ethanol (8 mL) was next added, followed by 3 M aqueous NaOH (1.86 mL) and finally 30% H₂O₂ (1.86 mL, slow addition). The resulting mixture was heated at 45 to 60 °C for 1 h. After being cooled to room temperature, the product mixture was diluted with water and extracted with ethyl acetate. The extracts were washed with water and brine, dried, and concentrated. Chromatography on silica gel (10% ethyl acetate in hexane) yielded alcohol **19** (0.36 g, 36%) as a colorless oil which was determined to be 86% ee (HPLC, *Chiralcel*, retention times 11.9 (R) and 6.6 min (S)): ¹H NMR (CDCl₃, 400 MHz) δ 7.30–7.16 (m, 5 H), 5.79 (dd, *J* = 17.3, 10.8 Hz, 1 H), 5.10–5.02 (m, 2 H), 3.27 (d, *J* = 10.8, 1 H), 2.96–2.85 (m, 1 H), 2.65–2.57 (m, 1 H), 1.87–1.79 (m, 1 H), 1.61–1.53 (m, 2 H), 0.99 (s, 6 H); [α]_D²⁵ +43.8° (c 1.0, MeOH).

(4R)-3,3-Dimethyl-6-phenyl-4-hex-1-enyl (2S)-1-(3,3-Dimethyl-1,2-dioxopentyl)-2-piperidinecarboxylate (7). A solution of (4R)-3,3-dimethyl-6-phenyl-1-hexen-4-ol (1.05 g, 5.15 mmol) in CH₂Cl₂ (100 mL) was treated with **30** (1.65 g, 6.47 mmol), DCC (2.75 g, 15.2 mmol), and DMAP (0.35 g, 2.87 mmol) to provide **7** (2.0 g, 88%) as a colorless oil: ¹H NMR (CDCl₃, 400 MHz, 6:1 mixture of trans-cis amide rotamers, data for trans rotamer) δ 7.29–7.15 (m, 5 H), 5.81 (dd, *J* = 17.2, 10.9 Hz, 1 H), 5.32 (d, *J* = 5.7 Hz, 1 H), 5.05–4.96 (m, 3 H), 3.42 (br d, *J* = 12.8 Hz, 1 H), 3.33 (td, *J* = 12.9, 3.3 Hz, 1 H), 2.70–2.45 (m, 3 H), 1.90–1.40 (m, 9 H), 1.25 (s, 3 H), 1.22 (s, 3 H), 1.03 (s, 3 H), 1.02 (s, 3 H), 0.90 (t, *J* = 7.6 Hz, 3 H); MS (DCI/NH₃), *m/z* 459 (M + NH₄)⁺. Anal. Calcd for C₂₇H₃₉NO₄: C, 73.43; H, 8.90; N, 3.17. Found: C, 73.18; H, 8.72; N, 3.15.

(1S)-1,3-Diphenyl-1-propanol (31) and (1R)-1,3-Diphenyl-1-propanol (20). A solution of (-)-*B*-chlorodiisopinocampheborane (0.70 g, 2.2 mmol) in THF (8.0 mL) was added to a solution of 1,3-diphenyl-1-propanone (0.43 g, 2.0 mmol) in THF (5.0 mL) and the resulting solution was allowed to stand overnight at -23 °C. The solvent was then evaporated. Diethyl ether (25 mL) and diethanolamine (0.40 g) were added and the resulting suspension was stirred for 3 h at room temperature. The mixture was then filtered and concentrated. Chromatography on silica gel (12% ethyl acetate in hexane) yielded (1S)-1,3-diphenyl-1-propanol (**31**, 0.25 g, 58%) as a white solid, which was recrystallized from hexane and found to be >99.9% ee by HPLC (*Chiralcel*, retention time 21.3 min for **31**, compared with 25.3 min for **20**): mp 49–50 °C; [α]_D²⁵ -14.8° (c 0.5, MeOH); ¹H NMR (CDCl₃, 400 MHz) δ 7.35–7.14 (m, 10 H), 4.65 (dd, *J* = 7.8, 5.4 Hz, 1 H), 2.78–2.59 (m, 2 H), 2.15–1.95 (m, 3 H); ¹³C NMR (CDCl₃, 100.6 MHz) δ 144.5, 142.0, 128.4, 127.7, 126.0, 74.1, 40.7, 32.0; IR (neat) 3600–3150 (br), 1600, 1490, 1450, 1215 cm⁻¹; MS (DCI/NH₃), *m/z* 230 (M + NH₄)⁺, 212. Anal. Calcd for C₁₅H₁₆O: C, 84.87; H, 7.60. Found: C, 84.74; H, 7.55.

An identical procedure except using (+)-*B*-chlorodiisopinocampheborane provided (1R)-1,3-diphenyl-1-propanol (**20**) with >99% ee (HPLC).

(1R)-1,3-Diphenyl-1-propyl (2S)-1-(3,3-Dimethyl-1,2-dioxopentyl)-2-piperidinecarboxylate (8). A solution of (1R)-1,3-diphenylpropanol

(62) Brown, H. C.; Singaram, B. *J. Org. Chem.* **1984**, *49*, 945–947.

(63) Jin, Y.-J.; Albers, M. W.; Lane, W. S.; Bierer, B. E.; Schreiber, S. L.; Burakoff, S. *J. Proc. Natl. Acad. Sci. U.S.A.* **1991**, *88*, 6677–6681.

(64) Galat, A.; Lane, W. S.; Standaert, R. F.; Schreiber, S. L. *Biochemistry* **1992**, *31*, 2427–2434.

(65) Jin, Y.-J.; Burakoff, S. J.; Bierer, B. E. *J. Biol. Chem.* **1992**, *267*, 10942–10945.

(66) Yem, A. W.; Tomasselli, A. G.; Heinrikson, R. L.; Zurcher-Neely, H.; Ruff, V. A.; Johnson, R. A.; Deibel, M. R., Jr. *J. Biol. Chem.* **1992**, *267*, 2868–2871.

(67) Tai, P.-K. K.; Albers, M. W.; Chang, H.; Faber, L. E.; Schreiber, S. L. *Science* **1992**, *256*, 1315–1318.

(68) Callebaut, I.; Renoir, J.-M.; Lebeau, M.-C.; Massol, N.; Burny, A.; Baulieu, E.-E.; Mornon, J.-P. *Proc. Natl. Acad. Sci. U.S.A.* **1992**, *89*, 6270–6274.

(80 mg, 0.37 mmol) in CH_2Cl_2 (1 mL) was treated with **30** (87 mg, 0.34 mmol), DCC (72 mg, 0.40 mmol), and DMAP (24 mg, 0.20 mmol) to provide **8** (100 mg, 67%) as a light yellow oil: $^1\text{H NMR}$ (CDCl_3 , 400 MHz, 5:1 mixture of trans-cis amide rotamers, data for trans rotamer) δ 7.35–7.13 (m, 10 H), 5.82 (dd, $J = 7.9, 6.0$ Hz, 1 H), 5.32 (d, $J = 4.7$ Hz, 1 H), 3.36 (br d, $J = 13.9$ Hz, 1 H), 3.13 (td, $J = 13.0, 3.1$ Hz, 1 H), 2.66–2.57 (m, 2 H), 2.35–2.28 (m, 2H), 2.13–2.07 (m, 1 H), 1.23 (s, 3 H), 1.20 (s, 3 H), 0.89 (t, $J = 7.5$ Hz, 3 H); MS (DCI/ NH_3), m/z 467 ($\text{M} + \text{NH}_4$)⁺. Anal. Calcd for $\text{C}_{28}\text{H}_{35}\text{NO}_4$: C, 74.80; H, 7.85; N, 3.12. Found: C, 74.31; H, 7.91; N, 3.05.

(1S)-1,3-Diphenyl-1-propyl (2S)-1-(3,3-Dimethyl-1,2-dioxopentyl)-2-piperidinecarboxylate (10). A solution of (1S)-1,3-diphenylpropanol (150 mg, 0.707 mmol) in CH_2Cl_2 (1 mL) was treated with **30** (100 mg, 0.392 mmol), DCC (130 mg, 0.630 mmol), DMAP (14.7 mg, 0.120 mmol), and CSA (28.0 mg, 0.121 mmol) to provide **10** (115 mg, 65%) as a light yellow oil: $^1\text{H NMR}$ (CDCl_3 , 400 MHz, 6:1 mixture of trans-cis amide rotamers, data for trans rotamer) δ 7.37–7.15 (m, 10 H), 5.77 (dd, $J = 7.8, 6.0$ Hz, 1 H), 5.30 (d, $J = 4.6$ Hz, 1 H), 3.36 (br d, $J = 12.8$ Hz, 1 H), 3.21 (td, $J = 12.9, 3.3$ Hz, 1 H), 2.70 (m, 2 H), 2.33–2.23 (m, 2 H), 2.16–2.08 (m, 1 H), 1.25 (s, 3 H), 1.20 (s, 3 H), 0.89 (t, $J = 7.5$ Hz, 3 H); $^{13}\text{C NMR}$ (CDCl_3 , 100.6 MHz) δ 207.9, 169.7, 166.6, 140.9, 140.1, 128.6, 128.5, 128.3, 128.1, 126.5, 126.3, 126.1, 76.9, 51.2, 43.9, 37.9, 32.5, 31.8, 26.4, 24.9, 23.7, 22.9, 20.9, 8.7; IR (neat) 2940, 1740, 1700, 1645, 1445, 1165, 990 cm^{-1} ; MS (DCI/ NH_3), m/z 467 ($\text{M} + \text{NH}_4$)⁺, 273, 212. Anal. Calcd for $\text{C}_{28}\text{H}_{35}\text{NO}_4$: C, 74.80; H, 7.85; N, 3.12. Found: C, 74.70; H, 7.92; N, 3.13.

(1R,S)-1-Cyclohexyl-3-phenyl-1-propanol (32). A solution of phenethyl bromide (3.7 g, 20 mmol) in diethyl ether (10 mL) was added to a rapidly stirred suspension of magnesium powder (0.53 g, 22 mmol) in ether (a few milliliters). Following the completion of addition, the resulting reflux was continued with external heating for 30 min. Cyclohexanecarboxaldehyde (2.24 g, 20 mmol) in ether (2 mL) was then added to the Grignard solution and heating was continued for an addition 30 min. The reaction mixture was then cooled to room temperature and poured into saturated aqueous NH_4Cl . The product was isolated by extraction with ethyl acetate and purified by chromatography on silica gel (10% ethyl acetate-hexane) to yield alcohol **32** (0.78 g, 18%) as a white solid: $^1\text{H NMR}$ (CDCl_3 , 400 MHz) δ 7.30–7.16 (m, 5 H), 3.4 (m, 1 H), 2.84–2.80 (m, 1 H), 2.69–2.63 (m, 1 H), 1.83–1.02 (m, 13 H).

(1R)-1-Cyclohexyl-3-phenyl-1-propyl (2S)-1-(3,3-Dimethyl-1,2-dioxopentyl)-2-piperidinecarboxylate (9) and **(1S)-1-Cyclohexyl-3-phenyl-1-propyl (2S)-1-(3,3-Dimethyl-1,2-dioxopentyl)-2-piperidinecarboxylate (11)**. A solution of (1R,S)-1-cyclohexyl-3-phenyl-1-propanol (**32**) (80 mg, 0.37 mmol) in CH_2Cl_2 (1.0 mL) was treated with **30** (87 mg, 0.34 mmol), DCC (72 mg, 0.40 mmol), and DMAP (24 mg, 0.20 mmol) to provide a mixture of **9** and **11** (75 mg, 48%) as a light yellow oil. MS (DCI/ NH_3), m/z 473 ($\text{M} + \text{NH}_4$)⁺, 456 ($\text{M} + \text{H}$)⁺. Anal. Calcd for $\text{C}_{28}\text{H}_{41}\text{NO}_4$: C, 73.81; H, 9.07; N, 3.07. Found: C, 73.61; H, 9.04; N, 2.98. Homogeneous **9** and **11** were obtained by preparative HPLC (*Chiracel*; 99.6% hexane, 0.2% 2-propanol, 0.2% ethanol; retention times 12.5 and 17.1 min, respectively). Data for **9**: $^1\text{H NMR}$ (CDCl_3 , 400 MHz, 5:1 mixture of trans-cis amide rotamers, data for trans rotamer) δ 7.28–7.15 (m, 5 H), 5.30 (d, $J = 4.7$ Hz, 1 H), 4.89 (dd, $J = 12, 6$ Hz, 1 H), 3.41 (br d, $J = 13$ Hz, 1 H), 3.28 (td, $J = 13, 3$ Hz, 1 H), 2.7–2.5 (m, 2 H), 2.34 (br d, $J = 12$ Hz, 2 H), 1.9–1.0 (m, 20 H), 1.25 (s, 3 H), 1.21 (s, 3 H), 0.90 (t, $J = 7.3$ Hz, 3 H); HRMS calcd for $\text{C}_{28}\text{H}_{41}\text{NO}_4\text{Na}$ ($\text{M} + \text{Na}$)⁺ 478.2933, found 478.2928. Data for **11**: $^1\text{H NMR}$ (CDCl_3 , 400 MHz, 5:1 mixture of trans-cis amide rotamers, data for trans rotamer) δ 7.30–7.15 (m, 5 H), 5.29 (d, $J = 4.7$ Hz, 1 H), 4.89 (dd, $J = 12, 6$ Hz, 1 H), 3.45 (br d, $J = 13$ Hz, 1 H), 3.27 (td, $J = 13.3$ Hz, 1 H), 2.75–2.55 (m, 2 H), 2.34 (br d, $J = 12$ Hz, 2 H), 1.95–1.0 (m, 20 H), 1.26 (s, 3 H), 1.22 (s, 3 H), 0.90 (t, $J = 7.3$ Hz, 3 H); HRMS calcd for $\text{C}_{28}\text{H}_{41}\text{NO}_4\text{Na}$ ($\text{M} + \text{Na}$)⁺ 478.2933, found 478.2941.

Benzyl 10-Hydroxydecanoate (33). A solution of 10-hydroxydecanoic acid (1.88 g, 10.0 mmol) in DMF (40 mL) was treated with potassium bicarbonate (1.1 g, 11.0 mmol) followed by benzyl bromide (1.97 g, 11.5 mmol) and was then stirred for 18 h at room temperature under argon. The solvent was evaporated under high vacuum and the residue was partitioned between ether and water. The aqueous layer was washed with ether and the combined organic extracts were dried over anhydrous magnesium sulfate. The resulting crude material was purified by silica gel flash chromatography (gradient elution with 20% to 30% ethyl acetate in hexane) to afford **33** (1.50 g, 54%) as a white solid: $^1\text{H NMR}$ (CDCl_3 , 250 MHz) δ 7.38–7.31 (m, 5 H), 5.11 (s, 2 H), 3.64 (t, $J = 6.6$ Hz, 2 H), 2.35 (t, $J = 7.5$ Hz, 2 H), 1.70–1.29 (m, 7 H); MS (DCI/ NH_3), m/z 296 ($\text{M} + \text{NH}_4$)⁺, 279.

Benzyl 12-Hydroxydecanoate (34). A solution of 12-hydroxydecanoic acid (2.16 g, 10.0 mmol) in DMF (40 mL) was treated with potassium bicarbonate (1.1 g, 11.0 mmol) and benzyl bromide (1.97 g, 11.5 mmol) at room temperature for 18 h to yield, after workup as above, **34** (2.14 g, 70%) as a white solid: $^1\text{H NMR}$ (CDCl_3 , 250 MHz) δ 7.38–7.31 (m, 5 H), 5.11 (s, 2 H), 3.64 (t, $J = 6.6$ Hz, 2 H), 2.35 (t, $J = 7.5$ Hz, 2 H), 1.67–1.26 (m, 9 H).

Ethyl (2S)-1-(3,3-Dimethyl-1,2-dioxo-4-hydroxybutyl)-2-piperidinecarboxylate (21). A mixture of ethyl L-pipecolate (3.0 g, 19.1 mmol), dihydro-4,4-dimethyl-2,3-furandione (2.57 g, 20.06 mmol), and DMAP (0.23 g, 1.9 mmol) in toluene (23 mL) was heated at reflux for 18 h under argon. The reaction mixture was concentrated under reduced pressure and the residue purified by silica gel flash chromatography (gradient elution with 10% to 30% ethyl acetate in hexane) to afford **21** (4.48 g, 82%) as a light yellow oil: $^1\text{H NMR}$ (CDCl_3 , 250 MHz, 6:1 mixture of trans-cis amide rotamers, data for trans rotamer) δ 5.25 (d, $J = 5.0$ Hz, 1 H), 4.25 (q, $J = 7.1$ Hz, 2 H), 3.68 (d, $J = 11.5$ Hz, 1 H), 3.60 (d, $J = 11.5$ Hz, 1 H), 3.50 (br d, $J = 13.1$ Hz, 1 H), 3.19 (td, $J = 13.0, 3.5$ Hz, 1 H), 2.35 (br d, $J = 14.0$ Hz, 1 H), 1.30 (t, $J = 7.1$ Hz, 3 H), 1.24 (s, 6 H); IR (neat) 3450 (br), 2950, 1745, 1705, 1635, 1450, 1210 cm^{-1} ; MS (DCI/ NH_3), m/z 303 ($\text{M} + \text{NH}_4$)⁺, 286, 273, 256, 210. Anal. Calcd for $\text{C}_{14}\text{H}_{23}\text{NO}_5 \cdot 0.3\text{H}_2\text{O}$: C, 57.87; H, 8.19; N, 4.82. Found: C, 57.80; H, 7.90; N, 5.09.

Ethyl (2S)-1-(4-((Benzoyloxy)methoxy)-3,3-dimethyl-1,2-dioxobutyl)-2-piperidinecarboxylate (35). Benzyl chloromethyl ether (5.26 g, 33.6 mmol) was added to a solution of alcohol **21** (4.0 g, 14.0 mmol) and *N,N*-diisopropylethylamine (23.0 g, 178 mmol) in CH_2Cl_2 (40 mL) and the resulting mixture was stirred at room temperature for 2 days under argon. The solvent was then evaporated under high vacuum and the residue was purified by silica gel flash chromatography (gradient elution with 2% to 10% ethyl acetate in hexane) to give **35** (5.03 g, 89%) as a colorless oil: $^1\text{H NMR}$ (CDCl_3 , 400 MHz, 4:1 mixture of trans-cis amide rotamers, data for trans rotamer) δ 7.37–7.28 (m, 5 H), 5.23 (d, $J = 5.5$ Hz, 1 H), 4.74 (s, 2 H), 4.59 (d, $J = 11.7$ Hz, 1 H), 4.56 (d, $J = 11.7$ Hz, 1 H), 4.22 (q, $J = 7.0$ Hz, 2 H), 3.81 (d, $J = 9.3$ Hz, 1 H), 3.61 (d, $J = 9.3$ Hz, 1 H), 3.58 (br d, $J = 13.0$ Hz, 1 H), 3.19 (td, $J = 13.1, 3.2$ Hz, 1 H), 2.31 (br d, $J = 13.9$ Hz, 1 H), 1.35 (s, 3 H), 1.31 (s, 3 H), 1.29 (t, $J = 7.0$ Hz, 3 H); IR (neat) 2950, 1745, 1715, 1645, 1450, 1210, 1055 cm^{-1} ; MS (DCI/ NH_3), m/z 423 ($\text{M} + \text{NH}_4$)⁺, 406, 331, 298. Anal. Calcd for $\text{C}_{22}\text{H}_{31}\text{NO}_6$: C, 65.17; H, 7.71; N, 3.45. Found: C, 64.87; H, 8.01; N, 3.58.

Ethyl (2S)-1-(4-(Tetrahydropyranloxy)-3,3-dimethyl-1,2-dioxobutyl)-2-piperidinecarboxylate (36). To a solution of ester **21** (9.6 g, 400 mmol) in THF (200 mL) was added 3,4-dihydro-2H-pyran (14.7 g, 800 mmol) and *p*-TsOH· H_2O (1.6 g, 100 mmol), and the resulting mixture was stirred at room temperature overnight. The mixture was then treated with NaHCO_3 (5 g), stirred for 2 h, filtered, and concentrated. Column chromatography on silica gel (20% EtOAc in hexanes) afforded **36** (7.8 g, 60%, mixture of acetal diastereomers) as a light yellow oil: $^1\text{H NMR}$ (CDCl_3 , 400 MHz, 4:1 mixture of trans-cis amide rotamers, data for trans rotamer) δ 5.25 (d, $J = 6.6$ Hz, 1 H), 4.60 (t, $J = 7.2$ Hz, 1 H), 4.3–4.5 (m, 1 H), 4.18 (q, $J = 7.2$ Hz, 2 H), 3.74–3.84 (m, 2 H), 3.65 (m, 2 H), 3.45 (m, 2 H), 3.15 (td, $J = 13.1, 3$ Hz, 1 H), 2.30 (br d, $J = 13.0$ Hz, 1 H), 1.35–1.75 (br m), 1.32 (s, 3 H), 1.25 (s, 3 H), 1.23 (t, $J = 7.2$ Hz, 3 H); $^{13}\text{C NMR}$ (CDCl_3 , 100.6 MHz) δ 170.2, 167.3, 98.6, 73.6, 62.2, 56.2, 51.4, 47.2, 43.6, 38.8, 30.6, 26.6, 25.5, 24.8, 23.5, 22.8, 21.4, 19.0, 14.4; IR (neat) 2940, 1740, 1710, 1640, 1450, 1370, 1340, 1280, 1250, 1200 cm^{-1} ; MS (DCI/ NH_3), m/z 354 ($\text{M} + \text{NH}_4$)⁺.

(2S)-1-(4-((Benzoyloxy)methoxy)-3,3-dimethyl-1,2-dioxobutyl)-2-piperidinecarboxylic Acid (22). A solution of ester **35** (4.6 g, 11.3 mmol) in methanol (124 mL) was treated with aqueous lithium hydroxide (0.678 g, 16.9 mmol in 74 mL of water) at 0 °C and the reaction mixture was stirred at room temperature for 3 h. Most of the methanol was then evaporated under reduced pressure and the resulting solution was partitioned between 1 N aqueous HCl and ethyl acetate. The aqueous layer was washed twice with ethyl acetate, and the combined organic extracts were dried over anhydrous magnesium sulfate and concentrated to afford **22** (4.2 g, 100%) as a white solid: $^1\text{H NMR}$ (CDCl_3 , 400 MHz, 4:1 mixture of trans-cis amide rotamers, data for trans rotamer) δ 7.37–7.28 (m, 5 H), 5.29 (d, $J = 5.2$ Hz, 1 H), 4.72 (s, 2 H), 4.59 (d, $J = 11.7$ Hz, 1 H), 4.55 (d, $J = 11.7$ Hz, 1 H), 3.77 (d, $J = 9.3$ Hz, 1 H), 3.64 (d, $J = 9.3$ Hz, 1 H), 3.59 (br d, $J = 13.0$ Hz, 1 H), 3.18 (td, $J = 13.0, 3.0$ Hz, 1 H), 2.33 (br d, $J = 13.9$ Hz, 1 H), 1.33 (s, 3 H), 1.30 (s, 3 H); MS (DCI/ NH_3), m/z 395 ($\text{M} + \text{NH}_4$)⁺, 378, 362, 334.

10-(Benzoyloxy)-10-oxo-1-decyl (2S)-1-(4-((Benzoyloxy)methoxy)-3,3-dimethyl-1,2-dioxobutyl)-2-piperidinecarboxylate (23). To a solution of carboxylic acid **22** (0.20 g, 0.53 mmol) and alcohol **33** (0.192 g, 0.69

mmol) in CH_2Cl_2 (1.4 mL) was added DCC (0.175 g, 0.85 mmol), DMAP (19 mg, 0.159 mmol), and CSA (37 mg, 0.159 mmol), and the resulting mixture was stirred for 18 h at room temperature. The mixture was then filtered through Celite, and the filter pad was rinsed with ethyl acetate. The filtrate was concentrated and the residue was purified by silica gel flash chromatography (gradient elution with 1% to 15% ethyl acetate in hexane) to give **23** (0.243 g, 72%) as a colorless oil: $^1\text{H NMR}$ (CDCl_3 , 250 MHz, 4:1 mixture of trans-cis amide rotamers, data for trans rotamer) δ 7.36–7.28 (m, 10 H), 5.23 (d, $J = 5.0$ Hz, 1 H), 5.11 (s, 2 H), 4.74 (s, 2 H), 4.59 (d, $J = 11.8$ Hz, 1 H), 4.55 (d, $J = 11.8$ Hz, 1 H), 4.14 (t, $J = 6.7$ Hz, 2 H), 3.79 (d, $J = 9.2$ Hz, 1 H), 3.62 (d, $J = 9.2$ Hz, 1 H), 3.57 (br d, $J = 13.0$ Hz, 1 H), 3.19 (td, $J = 13.0, 3.5$ Hz, 1 H), 2.35 (t, $J = 7.5$ Hz, 2 H), 2.30 (br d, $J = 13.5$ Hz, 1 H), 1.34 (s, 3 H), 1.31 (s, 3 H); IR (KBr) 2930, 1740, 1710, 1645, 1450, 1170, 1050 cm^{-1} ; MS (DCI/ NH_3), m/z 655 ($\text{M} + \text{NH}_4$) $^+$, 638, 530. Anal. Calcd for $\text{C}_{35}\text{H}_{51}\text{NO}_6$: C, 69.68; H, 8.06; N, 2.20. Found: C, 69.34; H, 7.79; N, 2.56.

12-(Benzyloxy)-12-oxo-1-dodecyl (2S)-1-(4-(Benzyloxy)methoxy)-3,3-dimethyl-1,2-dioxobutyl)-2-piperidinecarboxylate (24). A solution of acid **22** (0.20 g, 0.53 mmol), alcohol **34** (0.211 g, 0.69 mmol), DCC (0.175 g, 0.85 mmol), DMAP (19 mg, 0.159 mmol), and CSA (37 mg, 0.159 mmol) in CH_2Cl_2 (1.4 mL) was stirred for 18 h at room temperature. Workup as above afforded **24** (0.265 g, 75%) as a colorless oil: $^1\text{H NMR}$ (CDCl_3 , 400 MHz, 4:1 mixture of trans-cis amide rotamers, data for trans rotamer) δ 7.36–7.28 (m, 10 H), 5.23 (d, $J = 5.5$ Hz, 1 H), 5.11 (s, 2 H), 4.74 (s, 2 H), 4.59 (d, $J = 11.7$ Hz, 1 H), 4.55 (d, $J = 11.7$ Hz, 1 H), 4.17–4.09 (m, 2 H), 3.80 (d, $J = 9.3$ Hz, 1 H), 3.62 (d, $J = 9.3$ Hz, 1 H), 3.56 (br d, $J = 13.0$ Hz, 1 H), 3.20 (td, $J = 13.1, 3.2$ Hz, 1 H), 2.35 (t, $J = 7.5$ Hz, 2 H), 2.30 (br d, $J = 13.5$ Hz, 1 H), 1.35 (s, 3 H), 1.31 (s, 3 H); IR (KBr) 2940, 1745, 1715, 1645, 1455, 1170, 1055 cm^{-1} ; MS (DCI/ NH_3), m/z 683 ($\text{M} + \text{NH}_4$) $^+$, 666, 558, 468. Anal. Calcd for $\text{C}_{35}\text{H}_{53}\text{NO}_8$: C, 70.35; H, 8.33; N, 2.10. Found: C, 70.12; H, 8.14; N, 2.29.

10-Hydroxy-10-oxo-1-decyl (2S)-1-(3,3-Dimethyl-1,2-dioxo-4-hydroxybutyl)-2-piperidinecarboxylate (37). To a solution of **23** (0.21 g, 3.30 mmol) in 4:1 THF–water (26 mL) was added 10% palladium on activated carbon (0.108 g), and the resulting slurry was stirred under H_2 at room temperature for 3 h. Perchloric acid (0.05 N, 5.5 mL) was then added and stirring was continued for 18 h at room temperature. The mixture was filtered through Celite and the filter pad was rinsed with ethyl acetate. Most of the solvent was evaporated under reduced pressure and the resulting solution was partitioned between ethyl acetate and water. The layers were separated and the organic layer was washed with brine, dried over anhydrous sodium sulfate, and evaporated. The residue was purified by silica gel flash chromatography (elution with gradient 90:5:5 to 60:35:5 hexane–ethyl acetate–acetic acid) to provide **37** (103 mg, 74%) as a colorless oil: $^1\text{H NMR}$ (CDCl_3 , 250 MHz, 5:1 mixture of trans-cis amide rotamers, data for trans rotamer) δ 5.26 (d, $J = 5.2$ Hz, 1 H), 4.18 (t, $J = 6.5$ Hz, 2 H), 3.70 (d, $J = 11.8$ Hz, 1 H), 3.62 (d, $J = 11.5$ Hz, 1 H), 3.49 (br d, $J = 13.0$ Hz, 1 H), 3.19 (td, $J = 13.0, 3.3$ Hz, 1 H), 2.34 (t, $J = 7.5$ Hz, 2 H), 1.30 (s, 3 H), 1.24 (s, 3 H).

12-Hydroxy-12-oxo-1-dodecyl (2S)-1-(3,3-Dimethyl-1,2-dioxo-4-hydroxybutyl)-2-piperidinecarboxylate (38). To a solution of **24** (0.25 g, 0.375 mmol) in CH_2Cl_2 (4 mL) was added *N,N*-dimethylaniline (0.363 g, 3.0 mmol) followed by aluminum chloride (0.30 g, 2.25 mmol) at room temperature under argon. The reaction mixture turned green and was allowed to stir for 5 h at room temperature and then partitioned between ethyl acetate and 1 N aqueous HCl. The aqueous layer was separated and extracted twice with ethyl acetate. The combined organic extracts were washed with brine, dried over anhydrous sodium sulfate, and evaporated. The resulting crude material was purified by silica gel flash chromatography (elution with gradient 90:5:5 to 60:35:5 hexane–ethyl acetate–acetic acid) to provide **38** (75 mg, 44%) as a colorless oil: $^1\text{H NMR}$ (CDCl_3 , 250 MHz, 5:1 mixture of trans-cis amide rotamers, data for trans rotamer) δ 5.26 (d, $J = 5.1$ Hz, 1 H), 4.18 (t, $J = 6.7$ Hz, 2 H), 3.70 (d, $J = 11.5$ Hz, 1 H), 3.62 (d, $J = 11.5$ Hz, 1 H), 3.49 (br d, $J = 12.8$ Hz, 1 H), 3.19 (td, $J = 12.9, 3.3$ Hz, 1 H), 2.33 (t, $J = 7.5$ Hz, 2 H), 1.28 (s, 3 H), 1.24 (s, 3 H); IR (KBr) 3700–2400 (br), 2940, 1740, 1715, 1640, 1460, 1210, 1050 cm^{-1} ; MS (DCI/ NH_3), m/z 473 ($\text{M} + \text{NH}_4$) $^+$, 456.

(21S)-1-Aza-4,4-dimethyl-6,17-dioxo-2,3,7,18-tetraoxobicyclo[17.4.0]-tricosane (12). A mixture of hydroxy acid **37** (0.103 g, 0.241 mmol) and triethylamine (29.2 mg, 0.289 mmol) in anhydrous THF (4.7 mL) was stirred at room temperature for 10 min. 2,4,6-Trichlorobenzoyl chloride (64.4 mg, 0.264 mmol) was then added and stirring was continued for 2 h. The resulting mixture, containing the corresponding mixed anhydride, was diluted with toluene (118 mL) and added dropwise over 24 h by syringe pump to a refluxing solution of DMAP (0.734 g, 6.01 mmol) in

toluene (118 mL). The mixture was allowed to cool and was then successively washed with aqueous potassium bisulfate and brine and dried over anhydrous magnesium sulfate. The solvent was evaporated and the resulting crude material was purified by silica gel flash chromatography (gradient elution with toluene to 3% ethyl acetate in toluene) to give **12** (50 mg, 51%) as a white crystalline material: $^1\text{H NMR}$ (CDCl_3 , 400 MHz, 6:1 mixture of trans-cis amide rotamers, data for trans rotamer) δ 5.26 (d, $J = 5.5$ Hz, 1 H), 4.39 (dt, $J = 11.0, 6.0$ Hz, 1 H), 4.23 (s, 2 H), 4.08 (ddd, $J = 11.0, 6.0, 4.0$ Hz, 1 H), 3.60 (br d, $J = 12.8$ Hz, 1 H), 3.14 (td, $J = 12.9, 3.2$ Hz, 1 H), 2.35–2.25 (m, 2 H), 1.81 (br d, $J = 13.0$ Hz, 1 H), 1.36 (s, 3 H), 1.35 (s, 3 H); IR (CHCl_3) 2945, 1735, 1715, 1640 cm^{-1} ; MS (DCI/ NH_3), m/z 427 ($\text{M} + \text{NH}_4$) $^+$, 410. Anal. Calcd for $\text{C}_{22}\text{H}_{35}\text{NO}_6 \cdot 0.2\text{H}_2\text{O}$: C, 63.96; H, 8.64; N, 3.39. Found: C, 63.90; H, 8.52; N, 3.22.

(21S)-1-Aza-4,4-dimethyl-6,19-dioxo-2,3,7,20-tetraoxobicyclo[19.4.0]-pentacosane (13). A solution of hydroxy acid **37** (73 mg, 0.16 mmol) and triethylamine (19.4 mg, 0.19 mmol) in anhydrous THF (3.2 mL) was stirred at room temperature for 10 min as above. 2,4,6-Trichlorobenzoyl chloride (42.9 mg, 0.176 mmol) was then added and stirring was continued for 2 h. The reaction mixture was then diluted with toluene (79 mL) and added dropwise over 24 h to DMAP (0.488 g, 4.0 mmol) in refluxing toluene (79 mL). The reaction was worked up as above to provide **13** (36.5 mg, 52%) as a white crystalline material: $^1\text{H NMR}$ (CDCl_3 , 400 MHz, 6:1 mixture of trans-cis amide rotamers, data for trans rotamer) δ 5.26 (d, $J = 5.4$ Hz, 1 H), 4.34–4.14 (m, 2 H), 4.25 (d, $J = 10.9$ Hz, 1 H), 4.16 (d, $J = 10.9$ Hz, 1 H), 3.56 (br d, $J = 13.0$ Hz, 1 H), 3.15 (td, $J = 13.0, 3.2$ Hz, 1 H), 2.39 (br d, $J = 13.5$ Hz, 1 H), 2.34 (dt, $J = 15.0, 6.6$ Hz, 1 H), 2.26 (ddd, $J = 15.0, 8.4, 6.0$ Hz, 1 H), 1.81 (br d, $J = 13.0$ Hz, 1 H), 1.37 (s, 3 H), 1.35 (s, 3 H); MS (DCI/ NH_3), m/z 455 ($\text{M} + \text{NH}_4$) $^+$, 438, 224. Anal. Calcd for $\text{C}_{24}\text{H}_{39}\text{NO}_6$: C, 65.88; H, 8.98; N, 3.20. Found: C, 65.58; H, 9.12; N, 3.07.

3-Phenyl-1-(3-hydroxyphenyl)propanol (39). To a solution of 3-hydroxybenzaldehyde (9.0 g, 74 mmol) in THF (100 mL) was added 2-phenethylmagnesium bromide (1.5 M, 100 mL, 150 mmol) at -78°C under argon. The reaction mixture was stirred for 4 h at -78°C and then diluted with EtOAc (50 mL) and quenched with 1 N aqueous HCl (150 mL). The organic layer was dried, filtered, and concentrated *in vacuo*. Flash chromatography (silica gel, 20% EtOAc/hexanes) gave **39** (9.84 g, 58.3%) as a light yellow solid: mp 117–120 $^\circ\text{C}$; $^1\text{H NMR}$ (CDCl_3 , 400 MHz) δ 8.28 (s, 1 H), 7.2–6.7 (m, 9 H), 4.57 (t, $J = 6.1$ Hz, 1 H), 3.4 (s, 1 H), 2.70–2.59 (m, 2 H), 2.03–1.93 (m, 2 H); IR (KBr) 3450 (br), 2920, 1760, 1610, 1450, 1250 cm^{-1} ; MS (DCI/ NH_3), m/z 227 ($\text{M} + \text{NH}_4$) $^+$, 244. Anal. Calcd for $\text{C}_{15}\text{H}_{16}\text{O}_2$: C, 78.29; H, 7.06. Found: C, 78.69; H, 6.91.

3-Phenyl-1-(3-hydroxyphenyl)propan-1-one (40). A solution of alcohol **39** (2.0 g, 8.8 mmol) in acetone (20 mL) was treated with Jones reagent at room temperature until the yellow color persisted. The reaction was quenched with a few drops of 2-propanol, diluted with EtOAc, and extracted with H_2O . The organic layer was dried, filtered, concentrated *in vacuo*, and flash chromatographed (silica gel, 20% EtOAc/hexanes) to afford **40** (1.7 g, 84%) as a solid: mp 105–109 $^\circ\text{C}$; $^1\text{H NMR}$ (CDCl_3 , 400 MHz) δ 7.74–7.29 (m, 9 H), 3.51 (t, $J = 7.7$ Hz, 2 H), 3.30 (t, $J = 7.7$ Hz, 2 H); IR (KBr) 3450 (br), 2930, 1770, 1690, 1590, 1500, 1450, 1370, 1210 cm^{-1} ; MS (DCI/ NH_3), m/z 227 ($\text{M} + \text{NH}_4$) $^+$, 244. Anal. Calcd for $\text{C}_{15}\text{H}_{14}\text{O}_2$: C, 79.26; H, 6.65. Found: C, 78.97; H, 6.44.

3-Phenyl-1-(3-acetoxyphenyl)propan-1-one (41). To a solution of alcohol **40** (0.428 g, 1.9 mmol) in CH_2Cl_2 (2 mL) and pyridine 0.15 mL, 2 mmol) was added acetic anhydride (3 mL) at room temperature under argon, and the solution was then stirred for 4 h. The mixture was then diluted with CH_2Cl_2 (10 mL) and extracted with H_2O . The organic layer was dried, filtered, and concentrated *in vacuo* and flash chromatographed (silica gel, 20% EtOAc/hexanes) to afford **41** (460 mg, 90%) as a solid: mp 91–94 $^\circ\text{C}$; $^1\text{H NMR}$ (CDCl_3 , 400 MHz) δ 7.64–7.00 (m, 9 H), 3.09 (t, $J = 6.1$ Hz, 2 H), 2.87 (t, $J = 6.1$ Hz, 2 H), 2.13 (s, 3 H); IR (KBr) 2920, 1760, 1700, 1610, 1600, 1500, 1450, 1370, 1200 cm^{-1} ; MS (DCI/ NH_3), m/z 269 ($\text{M} + \text{NH}_4$) $^+$, 286. Anal. Calcd for $\text{C}_{17}\text{H}_{16}\text{O}_3$: C, 75.25; H, 7.05. Found: C, 75.18; H, 6.82.

(1R)-3-Phenyl-1-(3-acetoxyphenyl)propan-1-ol (42). A solution of **15** (0.268 g, 1.0 mmol) in THF (1 mL) was added dropwise to a solution of (+)-*B*-chlorodiisopinocampheylborane (2.24 g, 6.40 mmol) in THF (2 mL) at 0°C under argon and was allowed to stand overnight in a freezer at -23°C . The reaction mixture was then concentrated *in vacuo*, and the residue was redissolved in ether (25 mL) and treated with diethanolamine (0.35 g, 3 mmol) for 3 h at room temperature. The precipitate was removed by filtration, and the filtrate was concentrated *in vacuo* and purified by flash chromatography (silica gel, 20% EtOAc/hexanes) to afford **42** (227 mg, 84%) as a white solid: mp 120–124 $^\circ\text{C}$; $^1\text{H NMR}$

(CDCl₃, 400 MHz) δ 7.25–6.85 (m, 9 H), 4.57 (t, 1 H), 2.68–2.59 (m, 2 H), 2.2 (s, 3 H), 2.03–1.93 (m, 2 H); IR (KBr) 3400, 3030, 1760, 1590, 1480, 1400, 1260, 1150, 1050 cm⁻¹; MS (DCI/NH₃), m/z 271 (M + NH₄)⁺ 288. Anal. Calcd for C₁₇H₁₈O₃: C, 75.53; H, 6.71. Found: C, 75.18; H, 6.42.

(1R)-3-Phenyl-1-(3-hydroxyphenyl)propan-1-ol (43). A solution of sodium carbonate (0.1 g, 1 mmol) in H₂O (0.1 mL) was added to a solution of ester **42** (0.227 g, 0.84 mmol) in MeOH (4 mL) at 0 °C under argon and the solution was then stirred for 4 h. The mixture was diluted with CH₂Cl₂ (20 mL) and then acidified with 0.1 N aqueous HCl to pH 2. The organic layer was concentrated *in vacuo* and flash chromatographed (silica gel, 20% EtOAc/hexanes) to afford **43** (200 mg, 88%, 98% ee by Chiralcel HPLC) as a white solid: mp 102–105 °C; ¹H NMR (CDCl₃, 400 MHz) same as **2**; ¹³C NMR (CDCl₃, 100.6 MHz) δ 159.6, 146.0, 142.0, 129.2, 128.1, 125.5, 117.2, 114.3, 112.5, 73.2, 40.1, 31.8; MS (DCI/NH₃), m/z 229 (M + NH₄)⁺ 246; IR (KBr) 2920, 1772, 1680, 1590, 1500, 1450, 1370, 1220 cm⁻¹. Anal. Calcd for C₁₅H₁₆O₂: C, 78.92; H, 7.06. Found: C, 78.67, H, 6.75.

(1R)-3-Phenyl-1-(3-((7-*tert*-butoxy-7-oxoheptanyl)oxy)phenyl)propan-1-ol (25). Alcohol **43** (0.156 g, 0.69 mmol) was added to a mixture of NaH (17 mg) in DMSO (15 mL). *tert*-Butyl-1-bromoheptanoate (0.182 g, 0.69 mmol) was then added and the resulting mixture was stirred at 40 °C under argon overnight. The reaction was quenched with H₂O (20 mL) and the mixture was extracted with EtOAc and H₂O. The organic layer was dried, filtered, and concentrated *in vacuo*. Chromatography (silica gel, 30% EtOAc/hexanes) afforded **25** (195 mg, 68%) as a yellow oil: ¹H NMR (CDCl₃, 400 MHz) δ 6.71–7.22 (m, 9 H), 4.58 (t, 1 H), 3.87 (t, 2 H), 2.68–2.59 (m, 2 H), 2.14 (t, 1 H), 2.00–1.93 (m, 2 H), 1.57–1.50 (m, 2 H), 1.44–1.38 (m, 2 H), 1.36 (s, 9 H), 1.34–1.28 (m, 2 H); ¹³C NMR (CDCl₃, 100.6 MHz) δ 159.6, 146.0, 142.0, 129.4, 128.3, 125.7, 118.0, 113.5, 111.9, 79.5, 73.7, 67.7, 40.3, 35.4, 32.0, 29.0, 28.7, 28.0, 25.7, 24.9. MS (DCI/NH₃), m/z 413.4 (M + NH₄)⁺, 430.4; IR (neat) 3470, 2910, 1730, 1610, 1450, 1370, 1260, 1160 cm⁻¹. Anal. Calcd for C₂₆H₃₆O₄: C, 75.69; H, 8.80. Found: C, 75.24; H, 8.54.

(1R)-3-Phenyl-1-[3-((7-*tert*-butoxy-7-oxoheptanyl)oxy)phenyl]-1-propanyl (2S)-1-(2-(tetrahydropyranyl)-4-oxy-3,3-dimethyl-1,2-dioxobutyl)-2-piperidinecarboxylate (27). Lithium hydroxide (28 mg, 0.66 mmol) was added to a solution of ester **36** (200 mg, 0.58 mmol) in 5% H₂O/MeOH (5 mL) and the solution was stirred at room temperature for 2 h. The reaction mixture was concentrated *in vacuo*, and the residue was dissolved in THF (4 mL). Triethylamine (190 mg, 1.9 mmol) was added, followed by 2,4,6-trichlorobenzoyl chloride (150 mg, 0.6 mmol), and the mixture was stirred at room temperature for 1 h. A solution of alcohol **25** (224 mg, 0.58 mmol) in benzene (4 mL) was added to the mixture, followed by DMAP (150 mg, 1.2 mmol), and stirring was continued at room temperature overnight. The mixture was then filtered, concentrated *in vacuo*, and flash chromatographed (silica gel, 20% EtOAc/hexane) to afford **27** (152 mg, 36%) as a light yellow oil: ¹H NMR (CDCl₃, 400 MHz, 4:1 mixture of trans–cis amide rotamers, data for trans rotamer) δ 7.26–6.75 (m, 9 H), 5.75 (t, 1 H), 5.25 (d, J = 5.2 Hz, 1 H), 4.62 (t, J = 6.0 Hz, 1 H), 3.92 (t, J = 8.2 Hz, 2 H), 3.36 (br d, J = 13.0 Hz, 1 H), 3.21 (t, J = 9.2 Hz, 1 H), 2.67–2.59 (m, 2 H), 2.23–2.19 (t, J = 8.2 Hz, 2 H), 2.03–1.93 (m, 2 H), 1.75 (t, J = 14.2 Hz, 2 H), 1.60 (t, 2 H), 1.49–1.43 (m, 4 H), 1.41 (s, 9 H), 1.25 (s, 3 H), 1.20 (s, 3 H); ¹³C NMR (CDCl₃, 100.6 MHz) δ 174.2, 170.2, 167.2, 159.7, 141.3, 140.8, 128.4, 128.3, 126.0, 118.6, 114.2, 112.6, 99.2, 80.3, 73.4, 67.8, 62.2, 51.4, 47.1, 44.0, 38.0, 35.4, 31.5, 30.0, 29.1, 28.8, 28.1, 25.7, 25.3, 24.9, 22.8, 22.5, 19.0; MS (DCI/NH₃), m/z 736 (M + NH₄)⁺, 753; IR (neat) 3450, 2910, 1730, 1600, 1450, 1370, 1250, 1150 cm⁻¹. Anal. Calcd for C₄₃H₆₁O₉N: C, 70.18; H, 8.35; N, 1.90. Found: C, 70.12; H, 8.24; N, 2.19.

Macrocyclic 14. A solution of ester **27** (80 mg, 0.11 mmol) in CH₂Cl₂ (5.0 mL) was treated with trifluoroacetic acid (1.0 mL) and the mixture was stirred at room temperature for 1 h. The reaction mixture was diluted

with toluene (200 mL) and concentrated *in vacuo*. The residue was dissolved in MeOH (5 mL) and triethylamine (1 mL), and the solution was stirred for 2 h at room temperature and then filtered and concentrated *in vacuo*. The residue was dissolved in THF (2 mL) and triethylamine (0.015 mL, 0.1 mmol), 2,4,6-trichlorobenzoyl chloride (0.016 mL, 0.1 mmol) was added, and the resulting mixture was stirred at room temperature under argon for 2 h. The mixture was diluted with toluene (48 mL) and added dropwise over 24 h by syringe pump to a refluxing solution of DMAP (310 mg, 2.5 mmol) in toluene (50 mL). The mixture was cooled to room temperature and washed with aqueous potassium bisulfate and brine. The organic layer was dried, filtered, concentrated *in vacuo*, and purified by flash chromatography (silica gel, 20% EtOAc/hexanes) to afford **14** (24 mg, 55%) as a light yellow oil: ¹H NMR (CDCl₃, 400 MHz) δ 7.27–6.79 (m, 9 H), 5.80 (t, 1 H), 5.34 (d, J = 5.5 Hz, 1 H), 4.25 (d, J = 10.9 Hz, 1 H), 4.11 (d, J = 11 Hz, 1 H), 4.05 (tt, 1 H), 3.94 (tt, 1 H), 3.53 (brd, J = 11.8 Hz, 1 H), 2.92–2.98 (m, 1 H), 2.64–2.56 (m, 2 H), 2.37–2.30 (m, 2 H), 2.26–2.17 (m, 2 H), 2.09–2.06 (m, 1 H), 1.87–1.57 (m, 4 H), 1.42 (s, 3 H), 1.38 (s, 3 H); ¹³C NMR (CDCl₃, 100.6 MHz) δ 173.2, 169.4, 165.5, 159.5, 141.5, 140.4, 129.5, 128.3, 126.0, 120.0, 113.8, 112.2, 69.0, 67.3, 51.1, 43.9, 37.8, 33.3, 31.5, 28.4, 27.5, 25.0, 24.4, 22.2, 21.8, 20.8; IR (neat) 2930, 1740, 1640, 1600, 1450, 1320, 1250, 1200, 1150 cm⁻¹; MS (DCI/NH₃), m/z 578.4 (M + NH₄)⁺, 595. Anal. Calcd for C₃₄H₄₃O₇N: C, 70.68; H, 7.50; N, 2.42. Found: C, 70.96; H, 7.52; N, 2.11.

The macrocyclic diastereomer **15** was obtained by using racemic alcohol **39** instead of enantiomerically pure alcohol **43** in the same sequence of reactions leading to a mixture of diastereomeric macrocycles. Homogeneous **15** was obtained as an oil by HPLC (*Chiracel*) separation. ¹H NMR δ 7.35–6.80 (m, 9 H), 5.79 (t, J = 6.1 Hz, 1 H), 5.27 (d, J = 6.4 Hz, 1 H), 4.20 (dd, J = 10.5, 10.5 Hz, 2 H), 4.02 (t, J = 10.2 Hz, 2 H), 3.48 (br d, J = 12.9 Hz, 1 H), 3.16 (td, J = 12.9 Hz, 1 H), 2.68–2.60 (m, 2 H), 2.40–2.30 (m, 3 H), 2.28–2.20 (m, 2 H), 2.18–2.0 (m, 2 H), 1.86–1.52 (m, 6 H), 1.48 (s, 3 H), 1.28 (s, 3 H); IR (neat) 2920, 1740, 1640, 1610, 1450, 1320, 1250, 1200, 1150 cm⁻¹; MS (DCI/NH₃), 578 (M + NH₄)⁺, 595; HRMS calcd for C₃₄H₄₄N₇ (M + H)⁺ 578.3118, found 578.3134.

2-(3-Indolyl)ethyl (2S)-1-(3,3-Dimethyl-1,2-dioxopentyl)-2-piperidinecarboxylate (28). A solution of 3-indoleethanol (82 mg, 0.51 mmol) in CH₂Cl₂ (1.0 mL) was treated with **30** (100 mg, 0.392 mmol), DCC (129 mg, 0.627 mmol), DMAP (14.4 mg, 0.12 mmol), and CSA (27.3 mg, 0.118 mmol) to provide **28** (112 mg, 85%) as a colorless oil: ¹H NMR (CDCl₃, 400 MHz, 8:1 mixture of trans–cis amide rotamers, data for trans rotamer) δ 8.08 (br s), 7.61 (d, J = 7.8 Hz, 1 H), 7.37 (d, J = 8.0 Hz, 1 H), 7.21 (t, J = 7.6 Hz, 1 H), 7.13 (t, J = 7.4 Hz, 1 H), 7.09 (d, J = 1.8 Hz, 1 H), 5.27 (d, J = 5.1 Hz, 1 H), 4.49–4.41 (m, 2 H), 3.33 (br d, J = 13.0 Hz, 1 H), 3.20–3.07 (m, 3 H), 2.28 (d, J = 13.4 Hz, 1 H), 1.22 (s, 3 H), 1.18 (s, 3 H), 0.88 (t, J = 7.5 Hz, 3 H); MS (DCI/NH₃), m/z 416 (M + NH₄)⁺, 399. Anal. Calcd for C₂₃H₃₀N₂O₄: C, 69.32; H, 7.59; N, 7.03. Found: C, 69.31; H, 7.64; N, 6.46.

Acknowledgment. We are especially grateful to T. G. Porter and K. Kasyan for the supply of human recombinant FKBP12 used in this study, to M. Metzger, M. Huddleston, and W. Johnson for determination of mass spectra, to E. Reich for elemental analyses, and to K. Erhard for the skillful development of HPLC methods and purifications. Support from the NIH (CA-59021, J.C.) is gratefully acknowledged.

Supplementary Material Available: Tables of fractional atomic coordinates, anisotropic thermal parameters for non-hydrogen atoms, and tables containing additional metrical details for **13** (10 pages); listings of structure factors for **13** (32 pp). Ordering information is given on any current masthead page.